THE UNIVERSITY of EDINBURGH

Edinburgh Research Explorer

In situ cosmogenic nuclide production rate calibration for the CRONUS-Earth project from Lake Bonneville, Utah, shoreline features

Citation for published version:
Lifton, N, Caffee, M, Finkel, R, Marrero, S, Nishiizumi, K, Phillips, FM, Goehring, B, Gosse, J, Stone, J, Schaefer, J, Theriault, B, Jull, AJT & Fifield, K 2016, 'In situ cosmogenic nuclide production rate calibration for the CRONUS-Earth project from Lake Bonneville, Utah, shoreline features', *Quaternary Geochronology*, vol. 26, pp. 56-69. https://doi.org/10.1016/j.quageo.2014.11.002

Digital Object Identifier (DOI):
10.1016/j.quageo.2014.11.002

Link:
Link to publication record in Edinburgh Research Explorer

Document Version:
Peer reviewed version

Published In:
Quaternary Geochronology

Publisher Rights Statement:
Copyright © 2015 Elsevier B.V. All rights reserved.

General rights
Copyright for the publications made accessible via the Edinburgh Research Explorer is retained by the author(s) and / or other copyright owners and it is a condition of accessing these publications that users recognise and abide by the legal requirements associated with these rights.

Take down policy
The University of Edinburgh has made every reasonable effort to ensure that Edinburgh Research Explorer content complies with UK legislation. If you believe that the public display of this file breaches copyright please contact openaccess@ed.ac.uk providing details, and we will remove access to the work immediately and investigate your claim.

OPEN ACCESS

Download date: 05. May. 2023

Elsevier Editorial System(tm) for Quaternary Geochronology
Manuscript Draft

Manuscript Number: QUAGEO-D-14-00035R1

Title: In situ cosmogenic nuclide production rate calibration for the CRONUS-Earth Project from Lake Bonneville, Utah, shoreline features

Article Type: Special Issue: CRONUS-Earth volume

Keywords: cosmogenic nuclideproduction ratecalibrationinter-laboratory comparisonLake Bonneville historyberyllium-10aluminum-26carbon-14chlorine-36

Corresponding Author: Dr. Nathaniel Lifton, Ph.D.

Corresponding Author's Institution: Purdue University

First Author: Nathaniel Lifton, Ph.D.

Order of Authors: Nathaniel Lifton, Ph.D.; Marc Caffee, Ph.D.; Robert Finkel, Ph.D.; Shasta Marrero, Ph.D.; Kunihiko Nishiizumi, Ph.D.; Fred M Phillips, Ph.D.; Brent Goehring, Ph.D.; John Gosse, Ph.D.; John Stone, Ph.D.; Joerg Schaefer, Ph.D.; Bailey Theriault, M.S.; A. J. Timothy Jull, Ph.D.; Keith Fifield, Ph.D.

Abstract: Well-dated bedrock surfaces associated with the highstand and subsequent catastrophic draining of Pleistocene Lake Bonneville, Utah, during the Bonneville flood are excellent locations for in situ cosmogenic nuclide production rate calibration. The CRONUS-Earth Project sampled wave-polished bedrock and boulders on an extensive wave-cut bench formed during the Bonneville-level highstand that was abandoned almost instantaneously during the Bonneville flood. CRONUS-Earth also sampled the Tabernacle Hill basalt flow that erupted into Lake Bonneville soon after its stabilization at the Provo level, following the flood. New radiocarbon dating results from tufa at the margins of Tabernacle Hill as part of this study have solidified key aspects of the exposure history at both sites. Both sites have well-constrained exposure histories in which factors such as potential prior exposure, erosion, and shielding are either demonstrably negligible or quantifiable. Multi-nuclide analyses from multiple labs serve as an ad hoc inter-laboratory comparison that supplements and expands on the formalized CRONUS-Earth and CRONUS-EU inter-laboratory comparisons (Blard et al., 2014, this volume; Jull et al., 2013, this volume; Vermeesch et al., 2012, this volume). Results from 10Be, 26Al, and 14C all exhibit scatter comparable to that observed in the CRONUS-Earth effort. Although a 36Cl inter-laboratory comparison was not completed for Jull et al. (2013, this volume), 36Cl from plagioclase mineral separates exhibits comparable reproducibility. Site production rates derived from these measurements provide valuable input to the global production rate calibration described by Borchers et al. (in review, this volume). Whole-rock 36Cl concentrations, however, exhibit inter-laboratory variation exceeding analytical uncertainty and outside the ranges observed for the other nuclides (Jull et al., 2013, this volume). A rigorous inter-laboratory comparison studying the systematics of whole-rock 36Cl extraction techniques is currently underway with the goals of delineating the source(s) of this discrepancy and standardizing these procedures going forward.

*Manuscript
Click here to view linked References

In situ cosmogenic nuclide production rate calibration for the CRONUS-Earth Project from Lake Bonneville, Utah, shoreline features

Nathaniel Lifton[a,b], Marc Caffee[a,b], Robert Finkel[c], Shasta Marrero[d,f], Kunihiko Nishiizumi[e], Fred M. Phillips[f], Brent Goehring[g], John Gosse[h], John Stone[i], Joerg Schaefer[j], Bailey Theriault[k], A.J. Timothy Jull[l], Keith Fifield[m]

a *Corresponding Author*. Department of Earth, Atmospheric, and Planetary Sciences, Purdue University, 550 Stadium Mall Drive, West Lafayette, Indiana, 47907, USA. Phone: +1 765-494-0754. E-mail: nlifton@purdue.edu

b Department of Physics and Astronomy and Purdue Rare Isotope Measurement Laboratory (PRIME Lab), Purdue University, 525 Northwestern Avenue, West Lafayette, Indiana, 47907, USA. E-mail: mcaffee@purdue.edu

c Center for Accelerator Mass Spectrometry, Lawrence Livermore National Laboratory, P.O. Box 808, L-397, Livermore, CA, 94550, USA; rfinkel@berkeley.edu

d Currently: University of Edinburgh, Geography Building, Drummond Street, Edinburgh, EH8 9XP, UK. E-mail: shastamarrero@gmail.com

e Space Sciences Laboratory #7450, University of California, 7 Gauss Way, Berkeley, CA, 94720 USA. E-mail: kuni@ssl.berkeley.edu

f Department of Earth & Environmental Science, New Mexico Tech, 801 Leroy Place, Socorro, NM, 87801, USA. E-mail: phillips@nmt.edu

g Department of Earth and Environmental Sciences, Tulane University, 6823 St Charles Avenue, New Orleans, LA, 70118, USA. E-mail: bgoehrin@tulane.edu

h Department of Earth Sciences, Dalhousie University, PO Box 15000, Halifax, NS B3H 4R2, Canada. E-mail: john.gosse@Dal.Ca

i Department of Earth and Space Sciences, University of Washington, 4000 15th Avenue NE Seattle, WA, 98195, USA. E-mail: stone@geology.washington.edu

j Lamont-Doherty Earth Observatory, The Earth Institute at Columbia University, Route 9W, Palisades, NY, 10964, USA. E-mail: schaefer@ldeo.columbia.edu

k Golder Associates, 18300 NE Union Hill Road, Suite 200, Redmond, WA, 98052, USA

l Geosciences Department and Arizona Accelerator Mass Spectrometry Laboratory, University of Arizona, 1040 East 4th St, Tucson, Arizona, 85721, USA. E-mail: jull@email.arizona.edu

m Department of Nuclear Physics, Research School of Physical Sciences and Engineering, The Australian National University, Canberra, ACT 0200. E-mail: keith.fifield@anu.edu.au

Abstract

Well-dated bedrock surfaces associated with the highstand and subsequent catastrophic draining of Pleistocene Lake Bonneville, Utah, during the Bonneville flood are excellent locations for *in situ* cosmogenic nuclide production rate calibration. The CRONUS-Earth Project sampled wave-polished bedrock and boulders on an extensive wave-cut bench formed during the Bonneville-level highstand that was abandoned almost instantaneously during the Bonneville flood. CRONUS-Earth also sampled the Tabernacle Hill basalt flow that erupted into Lake Bonneville soon after its stabilization at the Provo level, following the flood. New radiocarbon dating results from tufa at the margins of Tabernacle Hill as part of this study have solidified key aspects of the exposure history at both sites. Both sites have well-constrained exposure histories in which factors such as potential prior exposure, erosion, and shielding are either demonstrably negligible or quantifiable. Multi-nuclide analyses from multiple labs serve as an ad hoc inter-laboratory comparison that supplements and expands on the formalized CRONUS-Earth and CRONUS-EU inter-laboratory comparisons (Blard et al., 2014, this volume; Jull et al., 2013, this volume; Vermeesch et al., 2012, this volume). Results from ^{10}Be, ^{26}Al, and ^{14}C all exhibit scatter comparable to that observed in the CRONUS-Earth effort. Although a ^{36}Cl inter-laboratory comparison was not completed for Jull et al. (2013, this volume), ^{36}Cl from plagioclase mineral separates exhibits comparable reproducibility. Site production rates derived from these measurements provide valuable input to the global production rate calibration described by Borchers et al. (in review, this volume). Whole-rock ^{36}Cl concentrations, however, exhibit inter-laboratory variation exceeding analytical uncertainty and outside the ranges observed for the other nuclides (Jull et al., 2013, this volume). A rigorous inter-laboratory comparison studying

the systematics of whole-rock ^{36}Cl extraction techniques is currently underway with the goals of delineating the source(s) of this discrepancy and standardizing these procedures going forward.

1.0 Introduction

Nuclide production rates are key parameters in the application of *in situ* cosmogenic nuclides; e.g., the accuracy of exposure ages is directly related to the accuracy of the production rates. The ability to infer temporal and spatial variation in production rates at a given location impacts the inferences that can be made using cosmogenic nuclide data. The goal of the CRONUS-Earth project is to improve our understanding of global cosmogenic nuclide production systematics. A major part of this effort is to derive cosmogenic nuclide production rates directly from measurements of samples collected from carefully selected sites with well-constrained exposure histories.

Well-dated bedrock surfaces in northwestern Utah and southern Idaho associated with Pleistocene Lake Bonneville provide a robust opportunity for cosmogenic nuclide production rate calibration (Oviatt et al., 1992). In the past, these surfaces were used to estimate late Quaternary production rates for several nuclides, including ^{3}He (Amidon and Farley, 2011; Cerling, 1990; Cerling and Craig, 1994; Goehring et al., 2010), ^{21}Ne (Poreda and Cerling, 1992), ^{10}Be (Gosse and Klein, 1996), ^{36}Cl (Phillips et al., 1996; Stone et al., 1996; Zreda et al., 1991), and ^{14}C (Handwerger et al., 1999; Lifton et al., 2001; Miller et al., 2006). To provide a basis for intercomparison between the production rates for commonly measured cosmogenic nuclides, and to ensure that the most current techniques are employed in both sampling and laboratory

77 procedures, key locations within the Lake Bonneville basin were re-sampled by CRONUS-Earth
78 (Fig. 1).

79 The lake-level chronology of Lake Bonneville is well constrained by numerous radiocarbon
80 ages (Reheis et al., 2014, and references therein). The Lake Bonneville highstand (known as the
81 Bonneville level) is well preserved as the Bonneville shoreline. This highstand is constrained in
82 age by several radiocarbon dates ranging between 18.9 and 18.0 cal ka, including new ones
83 generated during this study. The Bonneville shoreline is unique in that it was abandoned
84 essentially instantaneously due to a catastrophic failure of the lake threshold at Red Rock Pass in
85 southern Idaho, resulting in the Bonneville flood. The resulting ~100 m drop in lake level (model
86 altitudes from ca. 1552 m to ca. 1444 m, adjusted for isostatic rebound after the flood (Oviatt et
87 al., 1992; Reheis et al., 2014)) led to the formation of the Provo shoreline. CRONUS-Earth
88 targeted two features for sampling that are tied intimately to this history: a prominent cut
89 bedrock bench associated with the Bonneville shoreline at Promontory Point; and the Tabernacle
90 Hill basalt flow that erupted into the lake soon after stabilization at the Provo shoreline level
91 (Figs. 1 and 2). In this paper we discuss constraints on sample exposure history, present
92 analytical results from multiple laboratories for *in situ* ^{10}Be, ^{26}Al, ^{14}C, and ^{36}Cl and evaluate their
93 consistency, and present the cosmogenic nuclide site production rates derived from those results.

94 **2.0 History of Lake Bonneville**

95 Lake Bonneville was a large, closed-basin lake during the Late Pleistocene in the region that
96 is now occupied by the Great Salt Lake (Fig. 1); these features were first described by G.K.
97 Gilbert (Gilbert, 1890). The basin is characterized by a series of wave-cut bedrock benches and
98 depositional shoreline features that formed during stillstands of the lake. A detailed chronology

of the fluctuations of the lake level between 30 ^{14}C ka and 12 ^{14}C ka (33-12 cal ka BP) was presented by Oviatt et al. (1992) using more than 80 radiocarbon dates, and has been augmented more recently by others (e.g., Benson et al., 2011; Godsey et al., 2005; Godsey et al., 2011; Janecke and Oaks, 2011; McGee et al., 2012; Miller et al., 2012; Reheis et al., 2014; Sack, 1999) (Fig. 2).

The first transgression events in the recent paleolake history, between approximately 30 - 22 ^{14}C ka (30-25 cal ka BP), have little chronological information compared to the later phases (Oviatt et al., 1992). After a period of relatively shallow occupation, the lake levels rose relatively quickly from a low level, probably at or below the modern lake levels, to a mid-range lake level around 26.5 ^{14}C ka (ca. 29 cal ka BP). The lake level oscillated over a vertical distance of about 45 m between 22-20 ^{14}C ka (ca. 25-22 cal ka BP). The Stansbury shoreline was formed during these fluctuations, denoted the Stansbury oscillation (Fig. 2).

The final transgression leading to the Bonneville stage began around 20 ^{14}C ka (22 cal ka BP) (Oviatt et al., 1992). Based on lake cores, there were several smaller-scale (30-50 m) fluctuations in lake level during the transgression; none of these smaller fluctuations are evident in the shoreline record (Oviatt, 1997). At the end of this transgression, the lake reached its highest elevation at 1552 m (adjusted for isostatic rebound (Oviatt et al., 1992)). The highest shoreline, known as the Bonneville shoreline, formed at this elevation as the lake level stabilized (Oviatt et al., 1992). There is no evidence recognized within the Lake Bonneville basin for any prior occupation at or near the Bonneville shoreline level (e.g., Nishizawa et al., 2013; Reheis et al., 2014). At this time, the lake was large, having an area of more than 52,000 km^2 (Currey et al., 1984), and was ca. 350 m deep (Bills and May, 1987). The size and depth of the lake at this time allowed waves to be generated along the fetch of the lake. These waves had sufficient energy to

erode bedrock; they were able to cut deeply into the surrounding bedrock despite the relatively brief occupation of the shoreline (see below). Promontory Point is at the southern end of a narrow peninsula (actually an island during the Bonneville highstand – Fig. 1) extending from the northern lake margin into what was the deepest part of the lake, exposing bedrock on this peninsula to intense wave action. The.quartzite bedrock at the Bonneville level evinces the effects of the energy transported by these waves (Figs. 3 and 4).

A period of intermittent overflow at the alluvial fan threshold at Red Rock Pass near Zenda, Idaho continued for up to 500 years (Oviatt et al., 1992; Reheis et al., 2014). At the end of that period (detailed chronology discussed below), the alluvial fan sill at Red Rock Pass (Figs. 1 and 2) failed catastrophically and the Lake Bonneville flood inundated the Snake River plain to the north of the lake (Janecke and Oaks, 2011; Miller et al., 2012; Oviatt et al., 1992). During this flood event, the lake level rapidly dropped approximately 100 m, releasing ca. 4,750 km^3 of water (O'Connor, 1993). The lake level then stabilized at the elevation of a bedrock sill at Red Rock pass and the Provo level shoreline formed (Godsey et al., 2011; Janecke and Oaks, 2011; Miller et al., 2012; Oviatt et al., 1992) (Fig. 3). During this development, the intermittent overflow probably continued.

Current models of Provo-level history tend to favor approximately one to three thousand years of outflow with multiple minor shorelines reflecting changing outlet conditions at or near Red Rock Pass (Janecke and Oaks, 2011; Miller et al., 2012). However, the exposure history of the Tabernacle Hill basalt is unaffected by these minor fluctuations in lake level during Provo time. The eruption occurred very early in the Provo shoreline history and an eruption during the transgressive phase would have shown evidence of eventual cover by water from the Bonneville shoreline occupation.

2.1 Geochronological constraints on the Bonneville and Provo Shorelines

The chronology for the paleo-Lake Bonneville is considered to be one of the most reliable and robust in the world for a Pleistocene lake (Oviatt et al., 1992; Reheis et al., 2014). Although there are numerous independent ages (radiocarbon or other methods) providing constraints on lake levels since ca. 30 ^{14}C ka, there only are a few key groups of dates (discussed below) that delimit the particular events of interest to this study.

All original radiocarbon ages are reported as ^{14}C ka, indicating years before 1950, and have subsequently been converted to calendar years using Calib 6.02 (INTCAL09) (Reimer et al., 2009), reported as cal ka before present (BP = 1950) with ±1σ uncertainties. The cosmogenic nuclide calibration for CRONUS (Borchers et al., in review, this volume) used radiocarbon ages calibrated with this software. Since the cosmogenic nuclide calibration calculations were performed, however, a newer radiocarbon calibration curve has been published (INTCAL13) (Reimer et al., 2013). Calibrated radiocarbon ages in this study using INTCAL09 agree within ca. 100 years with those calibrated using INTCAL13 – as such they do not significantly affect the cosmogenic nuclide calibration (Borchers et al., in review, this volume). For consistency with the Brochers et al. (in review, this volume) calibration, we continue to cite calibrated radiocarbon ages using INTCAL09,; some ages are reported as " years before 2010" to indicate that 60 years has been added to the calibrated radiocarbon age**.**

The independent ages constraining the exposure age at Promontory Point, the end of the wave-cutting event and the abandonment of the shoreline, are based on the age of the Bonneville flood itself. The datasets that constrain this event include relevant ages from Oviatt et al. (1992), Oviatt and Nash (1989), and Reheis et al. (2014), new radiocarbon dates from nearshore gastropods (Miller et al., 2012), U/Th dates from carbonates in flooded cave deposits (McGee et

al., 2012), and CRONUS radiocarbon analyses from tufa samples collected from Tabernacle Hill (this study, below).

There are several radiocarbon ages constraining the time of occupation of the Bonneville shoreline, but the most reliable of these is from charcoal collected from a pre-Bonneville soil about 6 m below the highstand shoreline (Oviatt et al., 1992). This age (15.25 ± 0.16 ^{14}C ka; ETH-3518) marking the start of the Bonneville highstand calibrates to 18.5 ± 0.4 cal ka. There is no known shoreline evidence in the Bonneville basin for any earlier occupation of that level or higher (Oviatt et al., 1992; Reheis et al., 2014).

Miller et al. (2012) questioned the validity of dates on gastropods from Lake Bonneville based on new radiocarbon ages from the Provo shore zone that provide significantly older ages (18-17 cal ka) than corresponding shell radiocarbon ages from offshore sands (e.g., Godsey et al., 2005; Godsey et al., 2011) or sediment core total inorganic carbon (TIC) and δ^{18}O (Benson et al., 2011) (ca. 17-15 cal ka). Another new dataset (McGee et al., 2012) provides U/Th ages of carbonate deposits in caves of various altitudes in the Bonneville Lake area. The results indicate that carbonate deposition ceased at 18.12 ± 0.15 ka in a cave in the Fish Springs Range that is 40 m below the Bonneville shoreline highstand (McGee et al., 2012). By inference, this provides a minimum limiting age on the Bonneville flood. These new dates and questions about some of the original radiocarbon dates of Oviatt et al. (1992) and Oviatt and Nash (1989) led to an extensive reanalysis of the age of the Bonneville flood as part of the CRONUS initiative. This reanalysis included a focus on the Tabernacle Hill basalt flow – a locale of particular significance to the Bonneville flood chronology.

The Tabernacle Hill flow is a small (~ 17 km^2), circular basalt feature that erupted into pluvial Lake Bonneville when the lake level was at or near the Provo shoreline level, as indicated

191 by the presence of glassy basalt pillows, tufa, and beach deposits around the flow margins. There
192 is no evidence for submergence of the flow by Lake Bonneville. It is clear from pillow basalts
193 around the margin of the flow and other geologic evidence that the basalt erupted into a lake
194 approximately at the level of the Provo shoreline (Oviatt and Nash, 1989). However, the top of
195 the basalt flow shows no evidence of eruption into water, indicating that the eruption occurred
196 after the Bonneville flood event when the water was at the Provo shoreline level.

197 Tufa encrustations on the margins of the flow provide a radiocarbon constraint on the
198 youngest possible age of the basalt. A single radiocarbon date from this tufa of 17.3 ± 0.2 cal ka
199 before 2010 (14.3 ± 0.09 ^{14}C ka; Beta-23803) (Oviatt and Nash, 1989) has served as the most
200 direct constraint on the minimum age of the Bonneville Flood since it was first published. Given
201 the importance of this constraint, we collected 3 additional tufa samples from below the Provo
202 shoreline along the flow margin (Fig. 5; Table 1; Appendix 2) for radiocarbon analysis. Tufa
203 ages can be problematic due to recrystallization, so the new samples were collected from the
204 ceilings of shallow rock shelters. Because the tufa formed on a basalt, which contains no carbon,
205 the possibility of contamination from detrital carbon is low (Oviatt et al., 1992). McGee et al.
206 (2012) estimate radiocarbon reservoir effects in Lake Bonneville at < 200 years, so the calibrated
207 tufa ages should be representative of the formation age of the encrustations. The new tufa
208 samples were carefully treated using the procedure described in Appendix 3. The samples were
209 cut into stratigraphically oriented sections, with the ’top’ of each being younger and the ’bottom’
210 being older. Each of the 6 samples was then cleaned with Type-1 water, crushed, and sieved. The
211 samples were again cleaned with Type-1 water and then partially dissolved with HCl, following
212 a procedure modified from Oviatt and Nash (1989), prior to CO_2 extraction and graphitization for
213 analysis by AMS.

These six radiocarbon ages are presented in Table 1. The mean radiocarbon age is 14.9 ± 0.2 ^{14}C ka, which yields a calibrated age range of 18.2 ± 0.3 cal ka (CALIB 6.02). This is significantly older than the previous age assignment of Oviatt and Nash (1989). Since all evidence points to eruption into a Provo level lake, the flow has to be older than the tufa deposits and younger than the Bonneville Flood. The limited time period of tufa deposition on the flow margin early in the Provo history is consistent with the cave carbonate record of McGee et al. (2012), who attributed the observed hiatus in carbonate deposition between 18.1 ± 0.3 and 16.4 ± 0.2 ka (U-Th) to freshening of the lake from overflow at the Provo level and/or from post-flood mixing.

The new tufa ages provide the oldest post-flood constraints; however, the new post-flood ages overlap with the youngest pre-flood ages from recent studies (McGee et al., 2012; Miller et al., 2012; Reheis et al., 2014). Using only published pre-Bonneville ages from material other than shells, it seems clear that the new ages, including two different types of dating techniques, are consistent with an older age of the Bonneville flood than previously accepted (e.g., Lifton et al., 2001; Oviatt et al., 1992). Based on the overlap of the 2σ ranges of the new ages and the pre-Bonneville soil charcoal age, when considered with the U-series data of McGee et al. (2012), we place the age of the Bonneville Flood (and resulting abandonment of the Bonneville shoreline) at 18.36 ± 0.3 ka before 2010 (18.3 ± 0.3 cal ka BP), which we take as the exposure age of our samples at Promontory Point. Similarly, an age of 18.26 ± 0.3 ka before 2010 (18.2 ± 0.3 cal ka BP) is adopted for the Tabernacle Hill basalt flow.

3.0 Sampling Locations

3.1 Promontory Point

The cut bedrock benches at Promontory Point are among the largest in the Bonneville basin, measuring hundreds of meters in width, with approximately several dozen meters of overburden removed (based on topographic map estimates) (Figs. 3-5). These large-scale erosional features limit the possibility of significant cosmogenic nuclide inheritance. The surfaces are well preserved and exhibit primary wave-rounding/polishing. Quartzites and quartzite conglomerates of the late Precambrian Mutual Formation and the early Cambrian Tintic Quartzite Formation crop out at the site. Numerous joints within the quartzite likely facilitated the erosion (Lifton et al., 2001). Six samples from bedrock outcrops and large boulders exhibiting primary wave-polish were analyzed for ^{10}Be, ^{26}Al, and ^{14}C. The samples were collected with a rock saw, hammer, and chisel along a transect approximately perpendicular to the cut bedrock cliff face to test for any effects of differential shielding by overburden (Figs. 4-5). The sample locations, shielding, and other sample-specific information are included in Tables 2-3. Descriptions for each sample, including composition, and other important sample information have been included in Appendix 1.

3.2 Tabernacle Hill

Samples were collected from the north side of the volcanic cone to the east of a fissure-eruption tephra, shown on Figs. 6 and 7. The sampling sites were located within 500 m of each other in an attempt to obtain samples that would be uniform in composition and exposure history. Samples were collected from the tops of tumuli to eliminate topographic shielding corrections and to reduce the possibility of cover by soil or ash. Previous work by Stone et al. (1996) showed

little evidence of tephra cover. Eolian cover is a known problem for the western part of the flow, so this area was also avoided (C.G. Oviatt and D.M. Miller, 2005, personal communication). The samples were also taken well away from any edges formed by pressure ridges in order to reduce edge effects. A rock saw was used to make sure that samples were taken in the middle of the tumulus. Finally, the original surface texture of pahoehoe ropes (Marrero, 2009) was used to distinguish samples that had undergone very little erosion. Seven samples of the basalt were collected along with one tufa sample. Descriptions for each sample, including composition, and other important sample information have been included in Appendix 1.

4.0 Analytical Methods

Each rock sample was crushed to an appropriate size, homogenized at the Purdue Rare Isotope Measurement Laboratory (PRIME Lab) using multiple passes and recombinations through a riffle splitter, and then divided into smaller aliquots for distribution to multiple investigators for analysis. Analytical details for each nuclide are summarized below.

4.1 ^{10}Be, ^{26}Al

Quartz was extracted from each rock sample by selective dissolution of other minerals in dilute HF (Kohl and Nishiizumi, 1992), followed by flotation in dense liquids to remove HF-resistant heavy minerals. Chemical processing for ^{10}Be and ^{26}Al was carried out in four laboratories: Lamont-Doherty Earth Observatory (LDEO), Lawrence Livermore National Laboratory Center for Accelerator Mass Spectrometry (CAMS), Space Sciences Laboratory at the University of California at Berkeley (UCB), and the University of Washington (UW), following routine Be and Al isolation methods (e.g., Kohl and Nishiizumi, 1992, http://www.ldeo.columbia.edu/res/pi/tcn/LDEO_Cosmogenic_Nuclide_Lab/Chemistry.html,

http://depts.washington.edu/cosmolab/chem.html, http://www.physics.purdue.edu/primelab/AMSQAQC/BeAlPhyChmChart.pdf), ^{10}Be and ^{26}Al isotopic analyses were made at CAMS and the Purdue Rare Isotope Measurement Laboratory (PRIME Lab). Measured ^{10}Be/Be and ^{26}Al/Al ratios were blank-corrected and normalized to AMS standards (Nishiizumi, 2004; Nishiizumi et al., 2007).

4.2 In Situ ^{14}C

Pure quartz was isolated from each sample following the procedures modified from Kohl and Nishiizumi (1992), and pretreated for *in situ* ^{14}C analysis following Lifton et al. (2001) and Miller et al. (2006) using extraction systems at the University of Arizona (UA) and Lamont-Doherty Earth Observatory. *In situ* ^{14}C was extracted from each sample using techniques described by Lifton et al. (2001), Pigati et al.(2010), Miller et al. (2006), and Goehring et al. (2013). Two types of systems were used for extraction in this study: the recirculating system described by Lifton et al. (2001) and the flow-through system described by Pigati et al. (2010) and Goehring et al. (2013). The flow-through extraction system was used on all but two samples in this study (including those from the Lamont-Doherty lab); the remaining two samples were extracted using the recirculating system. The ^{14}C content of the samples was analyzed at the Arizona AMS Laboratory and blank-corrected following Lifton et al. (2001).

4.3 ^{36}Cl

Measurements of ^{36}Cl from Tabernacle Hill basalt were conducted by four laboratories: University of Washington (feldspar mineral separates), PRIME Lab (whole-rock), New Mexico Tech (NMT) (whole-rock and feldspar mineral separates), and Dalhousie University (Dal) (whole-rock). University of Washington analytical procedures were modified from Stone et al.

(1996), while those for the New Mexico Tech samples are presented in Marrero (2012). PRIME Lab analytical procedures were based on Sharma et al. (2000), while those at Dalhousie were adapted from the University of Washington laboratory (Evans et al., 1997; Stone et al., 1996). Blank-corrected ^{36}Cl measurements for the University of Washington were carried out at the AMS facility at the Australian National University, while those for PRIME Lab, New Mexico Tech, and Dalhousie were performed at PRIME Lab.

4.4 ^{3}He

He-3 analyses from the Tabernacle Hill basalt were conducted by Mark Kurz at the Woods Hole Oceanographic Institution. Methods and results are presented in Goehring et al. (2010) and are not repeated here.

5.0 Results

Although Jull et al. (2013, this volume) presented results from the inter-laboratory comparison undertaken as part of CRONUS-Earth, the Lake Bonneville sites provide an additional opportunity to study inter-laboratory variability due to the multiple labs preparing and analyzing samples from the locations described here. Below we present the results of these analyses organized by nuclide, with corresponding site production rates. All uncertainties are presented as 1σ, except as indicated.

5.1 ^{10}Be

The six Promontory Point samples were analyzed by four of the participating laboratories, with two (UW and LDEO) producing replicate analyses (Table 2, Fig. 8) – 39 analyses in total. Of the replicate analyses, LDEO performed three to four for each sample, while UW analyzed

two aliquots of two of the samples (05PPT-03 and 05PPT-05). Thickness- and shielding-corrected LDEO/CAMS ^{10}Be data show a small but consistently increasing trend between the earliest aliquots and those analyzed later, for all samples except 05PPT-05. The range of results for LDEO/CAMS for an individual sample exhibiting this trend is ca. 6-9% of the combined mean for all labs for that particular sample. Thickness- and shielding-corrected UW replicates are consistent with the other sample analyses except for the first aliquot of 05PPT-05, which was ca. 9% above the rest of the UW results. A replicate of that analysis on a new aliquot agrees with the other UW results, leaving the first result for that sample unexplained. Significantly, no significant trend, either sample-to-sample or between labs, is observed overall along the sampling transect (Fig. 8). Overall, the inverse error-weighted mean concentrations (thickness- and shielding-corrected) for each sample ranged from $2.63 \pm 0.04 \times 10^5$ at g^{-1} in sample 05PPT-02 to $2.84 \pm 0.05 \times 10^5$ at g^{-1} in 05PPT-05 (Table 2). Sample-specific inverse error-weighted means from the replicates agree within uncertainties with the corresponding weighted means pooled from all labs, supporting our pooled approach. The unweighted mean and standard deviation of the weighted mean ^{10}Be sample concentrations is $2.75 \pm 0.07 \times 10^5$ at g^{-1} (2.5%, MSWD = 3.7). Considered with the independent age of 18.36 ± 0.30 ka for the site, this yields a mean time-integrated site production rate of 15.1 ± 0.4 at g^{-1} y^{-1}. The coefficient of variation (COV – standard deviation divided by the mean) of that value (2.6%) is slightly better than the COV for the CRONUS-N inter-laboratory comparison sample (similar concentrations) described in Jull et al. (2013) (4.1%), and comparable to the COV for the high-concentration CRONUS-A sample (2.9%).

5.2 ^{26}Al

Three of the participating laboratories analyzed the Promontory Point samples for ^{26}Al: UW, LDEO, and UCB (Table 2, Fig. 9). All labs analyzed samples at CAMS, but UCB also had analyses done at PRIME Lab for comparison. Replicate analyses were only performed at UW on samples 05PPT-03 and 05PPT-05. Results agreed within 1σ analytical uncertainties. As with ^{10}Be, no significant trend was observed with distance along the transect from outermost (05PPT-04) to innermost (05PPT-08) sample (Fig. 9). Thickness- and shielding-corrected lab results for each sample generally agreed within analytical uncertainty, with the exception of LDEO for samples 05PPT-02 and 05PPT-03, which were significantly below results from the other labs (Table 2, Fig. 9). Inverse error-weighted means for each sample ranged from 1.59 ± 0.07 x 10^6 at g^{-1} for 05PPT-04 to 2.03 ± 0.12 x 10^6 at g^{-1} for 05PPT-03. The mean and standard deviation of the weighted mean ^{26}Al sample results is 1.83 ± 0.16 x 10^6 at g^{-1} (8.7%, MSWD = 6.5). This yields a mean time-integrated site production rate of 100.4 ± 9.0 at g^{-1} y^{-1}. The COV (9.0%) is comparable to the COV for the CRONUS-N inter-laboratory comparison sample described in Jull et al. (2013) (10.1%).

5.3 ^{14}C

Two labs analyzed the Promontory Point samples for *in situ* ^{14}C: UA and LDEO, although LDEO only analyzed 05PPT-01 and 05PPT-02 (Table 2, Fig. 10). UA performed replicate analyses for all samples except 05PPT-08. As with ^{10}Be and ^{26}Al, no significant trend was observed with distance along the transect from outermost (05PPT-04) to innermost (05PPT-08) sample (Fig. 10). Thickness- and shielding-corrected replicate results typically agreed within analytical uncertainties at 1-2σ. Inverse error-weighted means for each sample ranged from 3.49

364 ± 0.06 x 10^5 at g^{-1} for 05PPT-02 to 3.97 ± 0.13 x 10^5 at g^{-1} for 05PPT-05. The mean and standard
365 deviation of the weighted mean ^{14}C sample results for Promontory Point is 3.74 ± 0.17 x 10^5 at g^{-1}
366 (4.5%, MSWD = 5.3). This yields a mean time-integrated site production rate of 50.9 ± 2.4 at g^{-1} y^{-1}.
367 (4.7%). The COV (4.7%) is better than the COV for the CRONUS-A inter-laboratory
368 comparison sample described in Jull et al. (2013) (6.3%).

369 *5.4 ^{36}Cl*

370 Four labs processed Tabernacle Hill samples for ^{36}Cl. Five plagioclase mineral separates
371 were processed at UW. In addition to the CRONUS samples (05TAB-*XX* in Tables 3 and 4), the
372 UW lab also contributed analyses of five very similar mineral separate samples from a previous
373 sample collection trip to the same locality (TH-*X* in Tables 3 and 4). The other three labs, Dal,
374 PRIME, and NMT, processed whole-rock samples from Tabernacle Hill (Tables 5 and 6).

375 Replicates were run by UW on mineral separates from samples TH-2 and TH-3 – results for
376 each agreed within 1σ analytical uncertainties (Table 3). Thickness- and shielding-corrected
377 results for all mineral separates showed only slightly increased scatter, but all agreed within one
378 standard deviation of the mean value of 3.03 ± 0.11 x 10^5 at g^{-1} (3.7%, MSWD = 0.64) (Fig. 11).
379 Analyses of ^{36}Cl from mineral separates constrain the chemical composition of a sample to a
380 narrow range that is ideally dominated by one production pathway (e.g., Evans et al., 1997;
381 Schimmelpfennig et al., 2009; Schimmelpfennig et al., 2011; Stone et al., 1998; Stone et al.,
382 1996). As a result, the mineral separates were used as primary calibration samples for ^{36}Cl by
383 Borchers et al. (in review, this volume). Assuming essentially all production is from Ca, this
384 yields a mean time-integrated site production rate of 130.0 ± 5.9 at g^{-1} y^{-1}/g Ca (COV = 4.5%).

On the other hand, an assessment of consistency for whole-rock ^{36}Cl data is more complicated than for mineral separates, or for the other three nuclides measured for this paper, due to the strong compositional dependence of its overall production rate via several reaction mechanisms (e.g., Schimmelpfennig et al., 2009). As such, whole-rock ^{36}Cl analyses were only used to constrain thermal and epithermal neutron production parameters by Marrero et al. (in review).

It is reasonable to expect that if a rock sample is crushed and rigorously homogenized as was done for this study, and if multiple labs are given splits of the resulting rock powder and process that rock for whole-rock ^{36}Cl, each should expect to get similar concentrations of ^{36}Cl as a result. As shown in Fig. 11, that is clearly the case for two of the labs – Dal and PRIME, which agree within 1σ for 5 of 6 analyses. The third lab, NMT, produced results for the same samples that are consistently 25-30% higher on average than the results from the other two labs. NMT measured 2 replicates of 05TAB-01, and 3 replicates each of 05TAB-05, -06, and -07, with results generally agreeing within 1σ with the mean replicate value for each of those samples (Table 5, Fig. 11). We are not arguing here that one value or another is correct – indeed it is certainly possible that all are offset somehow from the "true" value of each sample. Instead, we are simply noting the disagreement between labs for a given sample that highlights the urgent need for an inter-laboratory comparison study similar to that presented in Jull et al. (this volume). While such a comparison was not completed for whole-rock ^{36}Cl as part of CRONUS-Earth, one currently underway using calcite and feldspar intercomparison materials generated by Tibor Dunai (University of Cologne) (Phillips et al., in preparation, this volume) hopefully will shed light on the analytical origins of this discrepancy. We also strongly suggest that the inclusion in such a study of homogenized whole-rock samples (such as those from Tabernacle Hill), spanning

a range of compositions, would provide critical additional constraints to whole-rock extraction systematics relative to data generated from mineral separates alone.

Fig. 12 presents an alternate view of the data in Fig. 11 in a format designed to investigate the potential effect of total chlorine concentrations (in parts per million, ppm) in the samples on ^{36}Cl production, and hence measured ^{36}Cl concentrations. Chlorine-36 concentrations are normalized by Ca content (in oxide weight percent) as nucleon spallation of Ca is expected to be the dominant production pathway in these rocks. In theory, all results should plot approximately co-linearly with the intercept for zero total Cl near the feldspar separate values (without adjusting for production from K – a minor component in these rocks). As expected, the mineral separates cluster at very low total Cl concentrations and a very limited range of [^{36}Cl]/[CaO]. The Dal and PRIME analyses still cluster separately from the NMT results, each on quasi-linear but somewhat different trends. On the whole, the NMT data reflect higher overall total Cl concentrations than the Dal and PRIME data. Given the rigorous homogenization procedures employed for these samples, we suggest that differences in ^{36}Cl concentrations for a given sample likely reflect differences in sample processing that influence the isotope dilution mass spectrometry analyses for both Cl and ^{36}Cl. As noted above, work to understand the sources of the observed analytical disagreement is ongoing.

6.0 Discussion

6.1 Site-Specific Considerations

The new age constraints on the timing of the Bonneville highstand and subsequent abandonment of the Bonneville shoreline resulting from the Bonneville flood provide a key part of the well-constrained exposure history required for a production rate calibration site. However,

both the Promontory Point and Tabernacle Hill sites have additional factors with the potential to affect measured concentrations and must be considered in assessing their suitability as calibration sites.

6.1.1 Promontory Point

There are two factors at Promontory Point that could potentially affect measured concentrations: surface erosion since exposure, and a remnant signal derived from prior exposure to cosmic rays (inheritance). We argue that the former is insignificant at this location, due to the well-preserved primary wave-rounded and polished surfaces on both the bedrock outcrops and boulders that were sampled. The potential for nuclide inheritance, however, deserves more consideration.

The samples from the Bonneville shoreline cut bench at Promontory Point conceivably could have experienced nuclide production at depth by muons under either rock or water, or both, prior to shoreline abandonment. Our sampling transect was specifically designed to allow us to recognize potential differences in subsurface muon production due to likely systematic thickening of overburden from the outboard margin of the bench toward the base of the cut cliff. Although accurate reconstruction of the pre-Bonneville shoreline topography is impossible, one can use existing topography to estimate plausible pre-shoreline configurations (and hence, potential overburden thicknesses) (Fig. 5). Plausible reconstructed overburden thicknesses over the samples from this analysis ranged from ca. 50 m to ca. 70 m from 05PPT-04 to 05PPT-08. For a quartzite density of 2.65 g cm^{-3}, this corresponds to mass depths of 13,250 and 18,550 g cm^{-2}. Assuming a fast muon attenuation length of 4320 g cm^{-2} (Heisinger et al., 2002a; Heisinger et al., 2002b), a conservative pre-Bonneville long-term erosion rate of 25 m/My (mean temperate climate value of Portenga and Bierman, 2011) and a pre-Bonneville equivalent exposure age of

453 10 Ma yields predicted concentrations of ^{10}Be of ca. 5600 at g^{-1} and 1600 at g^{-1} below 50 and 70
454 m of overburden, respectively. These values correspond to approximately 2% and 0.6% of the
455 mean measured ^{10}Be concentration, respectively. We consider these to be maximum values as
456 the ^{10}Be would be at secular equilibrium under these assumptions. Results for each nuclide
457 measured show no evidence of any systematic trend in concentration from the outermost sample
458 (05PPT-04) to the innermost (05PPT-08) (Figs. 4 and 8). Thus, while we cannot exclude
459 definitively that a minor portion of the measured concentrations may be derived from prior
460 subsurface production, we consider such effects unlikely.

461 Lifton et al. (2001) surveyed the elevations of estuarine deposits at the site relative to sample
462 locations similar to those of this study and concluded that the samples were submerged under ca.
463 17 m of water at the highest level of Lake Bonneville. Field evidence noted as part this study
464 suggests >10 m of water was present over the bench. Spallogenic neutrons are rapidly attenuated
465 with depth in water – assuming an effective attenuation length of 140 g cm^{-2}, 10-17 m of water
466 would lead to a reduction in nuclide production by spallation of approximately 4-5 orders of
467 magnitude over subaerial values. Combined with the brief duration of the occupation at the
468 Bonneville highstand (ca. 500-1000 years), and low surficial production rates from muons at the
469 site (ca. 0.2 at g^{-1} y^{-1} for ^{10}Be), we argue that subaqueous production is negligible.

470 6.1.2 Tabernacle Hill

471 At Tabernacle Hill, two factors that have the potential to affect measured concentrations in
472 the flow are surface erosion and ash cover..

473 Basalts erode through two distinct mechanisms: spalling of entire horizontal flow sheets and
474 gradual erosion. Pahoehoe flows can consist of a series of horizontal layers; spalling of the

surface layer reveals a new layer beneath that is essentially indistinguishable from the original surface (Cerling and Craig, 1994). These secondary surfaces can have pahoehoe ropes and other indications of an uneroded surface. Rubble around the pahoehoe outcrops might indicate that the surface isn't pristine. In the case of gradual erosion, the surface textures are worn down gradually through time. Pahoehoe ropes, glassy surface textures, or other indicators of an uneroded surface may be degraded or completely removed. In the case of a fresh basalt flow, the gradual erosion must first strip off the glassy, friable, outer layer until the denser, inner material is reached.

Erosion rates on basalts are difficult to quantify (Cerling, 1990). Cerling and Craig (1994) estimated that ropes cannot remain distinct with more than 1 cm of total erosion (a rate of 0.55 mm/kyr at Tabernacle Hill). On the other hand, Dunbar (1999) and Dunbar and Phillips (2004) estimated an erosion rate 5 mm/kyr, significantly higher, yielding ca. 8.5 cm of total erosion at Tabernacle Hill. It is possible that higher erosion rates are appropriate for younger samples until the outer, very friable layer is removed progressively, with erosion rates slowing significantly after the denser inner material is reached (Dunbar and Phillips 2004).

Based primarily on surface texture and lack of local rubble, none of the Tabernacle Hill samples experienced significant erosion in our judgment. It is likely that the actual erosion rate of the Tabernacle Hill basalt is closer to the lower bounding erosion rate discussed above than the upper. As such, an erosion rate of 1.0 ± 0.5 mm/kyr was assumed for the Tabernacle Hill samples. The uncertainty was set to half of the rate to account for the large possible range of erosion rates. Including this erosion rate has only a minimal effect on predicted production rates - within the uncertainty of the data.

Ash cover is possible in volcanic environments as a source of decreased cosmogenic production. This is especially worth consideration in this case because tuff cones such as those at Tabernacle Hill produce this ash as part of the eruption sequence (Oviatt and Nash, 1989). Although localized tephra from a fissure eruption is present in the vicinity of the samples, affected areas were specifically avoided during sampling. In addition, samples were taken at or near the tops of tumuli to avoid problems with accumulation of soil, ash, or other aeolian material. We consider ash cover as unlikely to have affected any of the samples considered here.

7.0 Conclusions

This study has demonstrated that well-dated bedrock surfaces associated with the catastrophic draining of Lake Bonneville in the Bonneville Flood – at Promontory Point and Tabernacle Hill – are excellent locations for *in situ* cosmogenic nuclide production rate calibration. New dating results from Tabernacle Hill as part of this study have solidified key aspects of the exposure history at both sites. As a result, both sites have well-constrained exposure histories in which factors such as potential prior exposure, erosion, and shielding are either demonstrably negligible or quantifiable. Multi-nuclide analyses from multiple labs serve as an ad hoc inter-laboratory comparison. Results from ^{10}Be, ^{26}Al, and ^{14}C all exhibit scatter comparable to that observed in the CRONUS-Earth and CRONUS-EU inter-laboratory comparisons (Jull et al., 2013, this volume; Vermeesch et al., 2012). Chlorine-36 from plagioclase mineral separates exhibits comparable reproducibility. Site production rates derived from these measurements provide valuable information for the global production rate calibration described by Borchers et al. (in review, this volume). Whole-rock ^{36}Cl analyses, however, exhibit inter-laboratory variation exceeding analytical uncertainty and outside the ranges observed for the other *in situ* cosmogenic nuclides (Jull et al., 2013, this volume). An inter-laboratory

comparison studying the systematics of whole-rock ^{36}Cl extraction techniques is currently underway using calcite and feldspar mineral separates. In our opinion, further study of homogenized whole-rock samples in the framework of a rigorous inter-laboratory comparison is also critical to understanding source(s) of this discrepancy and standardizing these procedures going forward.

Acknowledgements

The authors gratefully acknowledge support from NSF grants EAR-0345150 (Lifton), EAR-0345932 (Finkel), EAR-0345820 and EAR-1153689 (Caffee), EAR-0345949 (Phillips), EAR-0345574 (Stone), EAR-0345835 (Schaefer), and EAR-0345817 (Nishiizumi). We also thank Mr. John Young for allowing access to the Promontory Point site. Thure Cerling, Mark Kurz, Darryl Granger, and Terry Swanson helped to collect samples and provided valuable field insights. Adam Hudson processed the Tabernacle Hill tufas for radiocarbon dating, and Dylan Rood contributed significantly to sample analyses at CAMS. Finally, we thank P.H. Blard and an anonymous reviewer for thoughtful and thorough comments that greatly improved this manuscript.

References

Amidon, W.H., Farley, K.A., 2011. Cosmogenic ^{3}He production rates in apatite, zircon and pyroxene inferred from Bonneville flood erosional surfaces. Quaternary Geochronology 6, 10-21.

Benson, L.V., Lund, S.P., Smoot, J.P., Rhode, D.E., Spencer, R.J., Verosub, K.L., Louderback, L.A., Johnson, C.A., Rye, R.O., Negrini, R.M., 2011. The rise and fall of Lake Bonneville between 45 and 10.5 ka. Quaternary International 235, 57-69.

Bills, B., May, G., 1987. Lake Bonneville: Constraints on lithospheric thickness and upper mantle viscosity from isostatic warping of Bonneville, Provo, and Gilbert stage shorelines. Journal of Geophysical Research (ISSN 0148-0227).

Blard, P.-H., Balco, G., Burnard, P.G., Farley, K.A., Fenton, C.R., Friedrich, R., Jull, A.J.T., Niedermann, S., Pik, R., Schaefer, J.M., Scott, E.M., Shuster, D.L., Stuart, F.M., Stute, M., Tibari, B., Winckler, G., Zimmermann, L., 2014. An inter-laboratory comparison of cosmogenic ^{3}He and radiogenic ^{4}He in the CRONUS-P pyroxene standard. Quaternary Geochronology, 1-9.

Borchers, B., Marrero, S.M., Balco, G., Caffee, M., Goehring, B., Gosse, J., Kurz, M., Lifton, N., Nishiizumi, K., Phillips , F., Schaefer, J., Stone, J., in review. Geological calibration of spallation production rates in the CRONUS-Earth Project. Quaternary Geochronology, this volume.

Cerling, T., 1990. Dating geomorphologic surfaces using cosmogenic ^{3}He. Quaternary Research 33, 148-156.

Cerling, T., Craig, H., 1994. Cosmogenic ^{3}He production rates from 39 N to 46 N latitude, western USA and France. Geochimica Et Cosmochimica Acta 58, 249-255.

Currey, D., Atwood, G., Mabey, D., 1984. Major Levels of Great Salt Lake and Lake Bonneville. Utah Geological and Mineral Survey, p. Map 73.

Dunbar, N.W., 1999. Cosmogenic ^{36}Cl-determined age of the Carrizozo lava flows, south-central New Mexico. New Mexico Geology 21, 25-29.

562 Dunbar, N.W., Phillips , F.M., 2004. Cosmogenic ^{36}Cl ages of lava flows in the Zuni–Bandera
563 volcanic field, northcentral New Mexico, U.S.A. New Mexico Bureau of Geology and
564 Mineral Resources Bulletin, pp. 309-318.

565 Evans, J., Stone, J., Fifield, L., Cresswell, R., 1997. Cosmogenic chlorine-36 production in K-
566 feldspar. Nuclear Instruments and Methods in Phys Res-Section B Only-Beam Interact
567 Mater Atoms 123, 334-340.

568 Gilbert, G.K., 1890. Lake Bonneville. United States Geological Survey Monograph, Washington,
569 D.C., p. 438.

570 Godsey, H., Currey, D., Chan, M., 2005. New evidence for an extended occupation of the Provo
571 shoreline and implications for regional climate change, Pleistocene Lake Bonneville, Utah,
572 USA. Quaternary Research 63, 212-223.

573 Godsey, H.S., Oviatt, C.G., Miller, D.M., Chan, M.A., 2011. Stratigraphy and chronology of
574 offshore to nearshore deposits associated with the Provo shoreline, Pleistocene Lake
575 Bonneville, Utah. Palaeogeography, Palaeoclimatology, Palaeoecology 310, 442-450.

576 Goehring, B.M., Kurz, M.D., Balco, G., Schaefer, J.M., Licciardi, J., Lifton, N., 2010. A
577 reevaluation of in situ cosmogenic ^{3}He production rates. Quaternary Geochronology 5,
578 410-418.

579 Goehring, B.M., Schimmelpfennig, I., Schaefer, J.M., 2013. Capabilities of the Lamont-Doherty
580 Earth Observatory in situ ^{14}C extraction laboratory updated. Quaternary Geochronology, 1-
581 18.

582 Gosse, J., Klein, J., 1996. Production rate of in situ cosmogenic ^{10}Be in quartz at high altitude
583 and mid latitude. Radiocarbon 38, 154-155.

584 Handwerger, D., Cerling, T., Bruhn, R., 1999. Cosmogenic ^{14}C in carbonate rocks.
585 Geomorphology 27, 13-24.

586 Heisinger, B., Lal, D., Jull, A., Kubik, P., Ivy-Ochs, S., Knie, K., Nolte, E., 2002a. Production of
587 selected cosmogenic radionuclides by muons: 2. Capture of negative muons. Earth and
588 Planetary Science Letters 200, 357-369.

589 Heisinger, B., Lal, D., Jull, A., Kubik, P., Ivy-Ochs, S., Neumaier, S., Knie, K., Lazarev, V.,
590 Nolte, E., 2002b. Production of selected cosmogenic radionuclides by muons 1. Fast
591 muons. Earth and Planetary Science Letters 200, 345-355.

592 Janecke, S.U., Oaks, R.Q., 2011. New insights into the outlet conditions of late Pleistocene Lake
593 Bonneville, southeastern Idaho, USA. Geosphere 7, 1369-1391.

594 Jull, A.J.T., Scott, E.M., Bierman, P., 2013. The CRONUS-Earth inter-comparison for
595 cosmogenic isotope analysis. Quaternary Geochronology, 1-8.

596 Kohl, C., Nishiizumi, K., 1992. Chemical isolation of quartz for measurement of in-situ-
597 produced cosmogenic nuclides. Geochimica Et Cosmochimica Acta 56, 3583-3587.

598 Lifton, N., Jull, A., Quade, J., 2001. A new extraction technique and production rate estimate for
599 in situ cosmogenic ^{14}C in quartz. Geochimica Et Cosmochimica Acta 65, 1953-1969.

600 Marrero, S., 2009. Chlorine-36 Prodcution Rate Calibration Using Shorelines from Pleistocene
601 Lake Bonneville, UT, Earth and Environmental Science. New Mexico Tech, Socorro, New
602 Mexico.

603 Marrero, S., 2012. Calibration of cosmogenic chlorine-36, Earth and Environmental Science
604 Dept. . New Mexico Tech, Socorro, NM.

Marrero, S.M., Phillips , F.M., Caffee, M., Gosse, J., in review. CRONUS-Earth cosmogenic ^{36}Cl calibration. Quaternary Geochronology, this volume.

McGee, D., Quade, J., Edwards, R.L., Broecker, W.S., Cheng, H., Reiners, P.W., Evenson, N., 2012. Lacustrine cave carbonates Novel archives of paleohydrologic change in the Bonneville Basin (Utah, USA). Earth and Planetary Science Letters 351-352, 182-194.

Miller, D.M., Oviatt, C.G., Mcgeehin, J.P., 2012. Stratigraphy and chronology of Provo shoreline deposits and lake-level implications, Late Pleistocene Lake Bonneville, eastern Great Basin, USA. Boreas 42, 342-361.

Miller, G., Briner, J., Lifton, N., Finkel, R.C., 2006. Limited ice-sheet erosion and complex exposure histories derived from in situ cosmogenic ^{10}Be, ^{26}Al, and ^{14}C on Baffin Island, Arctic Canada. Quaternary Geochronology 1, 74-85.

Nishiizumi, K., 2004. Preparation of ^{26}Al AMS standards. Nuclear Instruments and Methods in Physics Research Section B 223, 388-392.

Nishiizumi, K., Imamura, M., Caffee, M., Southon, J., Finkel, R.C., Mcaninch, J., 2007. Absolute calibration of ^{10}Be AMS standards. Nuclear Instruments and Methods in Physics Research Section B: Beam Interactions with Materials and Atoms 258, 403-413.

Nishizawa, S., Currey, D.R., Brunelle, A., Sack, D., 2013. Bonneville basin shoreline records of large lake intervals during Marine Isotope Stage 3 and the Last Glacial Maximum. Palaeogeography, Palaeoclimatology, Palaeoecology 386, 374-391.

O'Connor, J., 1993. Hydrology, hydraulics, and geomorphology of the Bonneville flood, Special Paper. Geological Society of America, p. 83.

Oviatt, C., 1997. Lake Bonneville fluctuations and global climate change. Geology 25, 155-158.

627 Oviatt, C., Currey, D., Sack, D., 1992. Radiocarbon chronology of Lake Bonneville, eastern
628 Great Basin, USA. Palaeogeography, Palaeoclimatology, Palaeoecology 99, 225-241.

629 Oviatt, C., Nash, W., 1989. Late Pleistocene basaltic ash and volcanic eruptions in the
630 Bonneville basin, Utah. Bulletin of the Geological Society of America 101, 292-303.

631 Phillips, F., Zreda, M., Flinsch, M., Elmore, D., Sharma, P., 1996. A reevaluation of cosmogenic
632 ^{36}Cl production rates in terrestrial rocks. Geophysical Research Letters 23.

633 Phillips, F.M., Argento, D.C., Balco, G., Caffee, M.W., Clem, J., Dunai, T., Finkel, R.,
634 Goehring, B., Gosse, J.C., Hudson, A., Jull, A.J.T., Kelly, M., Kurz, M.D., Lal, D., Lifton,
635 N., Marrero, S.M., Nishiizumi, K., Reedy, R., Schaefer, J., Stone, J.O.H., Swanson, T.,
636 Zreda, M.G., in preparation. The CRONUS-Earth Project: A synthesis. Quaternary
637 Geochronology, this volume.

638 Pigati, J., Lifton, N., Jull, A., Quade, J., 2010. A simplified in situ cosmogenic ^{14}C extraction
639 system. Radiocarbon 52, 1236-1243.

640 Poreda, R., Cerling, T., 1992. Cosmogenic neon in recent lavas from the western United States.
641 Geophysical Research Letters 19, 1863-1866.

642 Portenga, E.W., Bierman, P.R., 2011. Understanding Earth's eroding surface with ^{10}Be. GSA
643 Today 21, 4-10.

644 Reheis, M.C., Adams, K.D., Oviatt, C.G., Bacon, S.N., 2014. Pluvial lakes in the Great Basin of
645 the western United States-a view from the outcrop. Quaternary Science Reviews 97, 33-57.

646 Reimer, P., Baillie, M., Bard, E., Bayliss, A., Beck, J., Blackwell, P., Bronk Ramsey, C., Buck,
647 C., Burr, G., Edwards, R., Friedrich, M., Grootes, P., Guilderson, T., Hajdas, I., Heaton, T.,
648 Hogg, A., Hughen, K., Kaiser, K., Kromer, B., McCormac, F., Manning, S., Reimer, R.,

649 Richards, D., Southon, J., Talamo, S., Turney, C., van der Plicht, J., Weyhenmeyer, C.,
650 2009. IntCal09 and Marine09 radiocarbon age calibration curves, 0–50,000 years cal BP.
651 Radiocarbon 51, 1111-1150.

652 Reimer, P.J., Bard, E., Bayliss, A., Beck, J.W., Blackwell, P.G., Ramsey, C.B., Buck, C.E.,
653 Cheng, H., Edwards, R.L., Friedrich, M., Grootes, P.M., Guilderson, T.P., Haflidason, H.,
654 Hajdas, I., Hatté, C., Heaton, T.J., Hoffmann, D.L., Hogg, A.G., Hughen, K.A., Kaiser,
655 K.F., Kromer, B., Manning, S.W., Niu, M., Reimer, R.W., Richards, D.A., Scott, E.M.,
656 Southon, J.R., Staff, R.A., Turney, C.S.M., van der Plicht, J., 2013. IntCal13 and Marine13
657 radiocarbon age calibration curves 0–50,000 years cal BP. Radiocarbon 55, 1869-1887.

658 Sack, D., 1999. The composite nature of the Provo level of Lake Bonneville, Great Basin,
659 western North America. Quaternary Research 52, 316-327.

660 Schimmelpfennig, I., Benedetti, L., Finkel, R., Pik, R., Blard, P.-H., Bourles, D., Burnard, P.,
661 Williams, A., 2009. Sources of in-situ ^{36}Cl in basaltic rocks. Implications for calibration of
662 production rates. Quaternary Geochronology 4, 441-461.

663 Schimmelpfennig, I., Benedetti, L., Garreta, V., Pik, R., Blard, P.-H., Burnard, P., Bourlès, D.,
664 Finkel, R., Ammon, K., Dunai, T., 2011. Calibration of cosmogenic ^{36}Cl production rates
665 from Ca and K spallation in lava flows from Mt. Etna (38°N, Italy) and Payun Matru
666 (36°S, Argentina). Geochimica Et Cosmochimica Acta 75, 2611-2632.

667 Sharma, P., Bourgeois, M., Elmore, D., Granger, D., Lipschutz, M.E., Ma, X., Miller, T.,
668 Mueller, K., Rickey, F., Simms, P., Vogt, S., 2000. PRIME lab AMS performance,
669 upgrades and research applications. Nuclear Instrumentrs and Methods in Physics Research
670 B 172, 112-123.

671 Stone, J., Evans, J., Fifield, L., Allan, G., Cresswell, R., 1998. Cosmogenic Chlorine-36
672 Production in Calcite by Muons. Geochimica Et Cosmochimica Acta 62, 433-454.

673 Stone, J.O., Allan, G.L., Fifield, L.K., Cresswell, R.G., 1996. Cosmogenic chlorine-36 from
674 calcium spallation. Geochimica Et Cosmochimica Acta 60, 679-692.

675 Vermeesch, P., Balco, G., Blard, P.-H., Dunai, T.J., Kober, F., Niedermann, S., Shuster, D.L.,
676 Strasky, S., Stuart, F.M., Wieler, R., Zimmermann, L., 2012. Interlaboratory comparison of
677 cosmogenic ^{21}Ne in quartz. Quaternary Geochronology, 1-9.

678 Zreda, M.G., Phillips, F.M., Elmore, D., Kubik, P.W., Sharma, P., Dorn, R.I., 1991. Cosmogenic
679 chlorine-36 production rates in terrestrial rocks. Earth and Planetary Science Letters 105,
680 94-109.

681

List of Figures

locations are shown as black dots in the image on the right. Samples were collected in a transect stretching from the cliff to the far end of the bench (Marrero, 2012).

Figure 6: A. Google Earth image of Tabernacle Hill showing the whole flow and the area in which the samples were collected (black rectangle). The black oval indicates the tufa sampling location. B. Closeup of the sampling area showing individual sample locations and other features, such as the Provo shoreline (altitude ca. 1440 m), wave-cut platform, and the tephra deposit.

Figure 7: Photo looking south from the sampled northern portion of the Tabernacle Hill basalt flow toward the central cinder cone. Note prominent tumuli (pressure ridges).

Figure 8: Measured ^{10}Be concentrations corrected to zero thickness, horizontal orientation, and no topographic shielding. Mean and standard deviation of measurements shown as purple line and shading. Lab abbreviations given in text.

Figure 9: Measured ^{26}Al concentrations corrected to zero thickness, horizontal orientation, and no topographic shielding. Mean and standard deviation of measurements shown as purple line and shading. Lab abbreviations given in text.

Figure 10: Measured ^{14}C concentrations corrected to zero thickness, horizontal orientation, and no topographic shielding. Mean and standard deviation of measurements shown as purple line and shading. Lab abbreviations given in text.

Figure 11: Measured ^{36}Cl concentrations. Mean and standard deviation of plagioclase mineral separate measurements shown as purple line and shading. Lab abbreviations given in text.

Figure 12: Measured ^{36}Cl concentrations normalized to CaO concentration (in plagioclase for mineral separates, bulk rock for whole-rock), plotted vs. corresponding total Cl concentration.

Figure 1

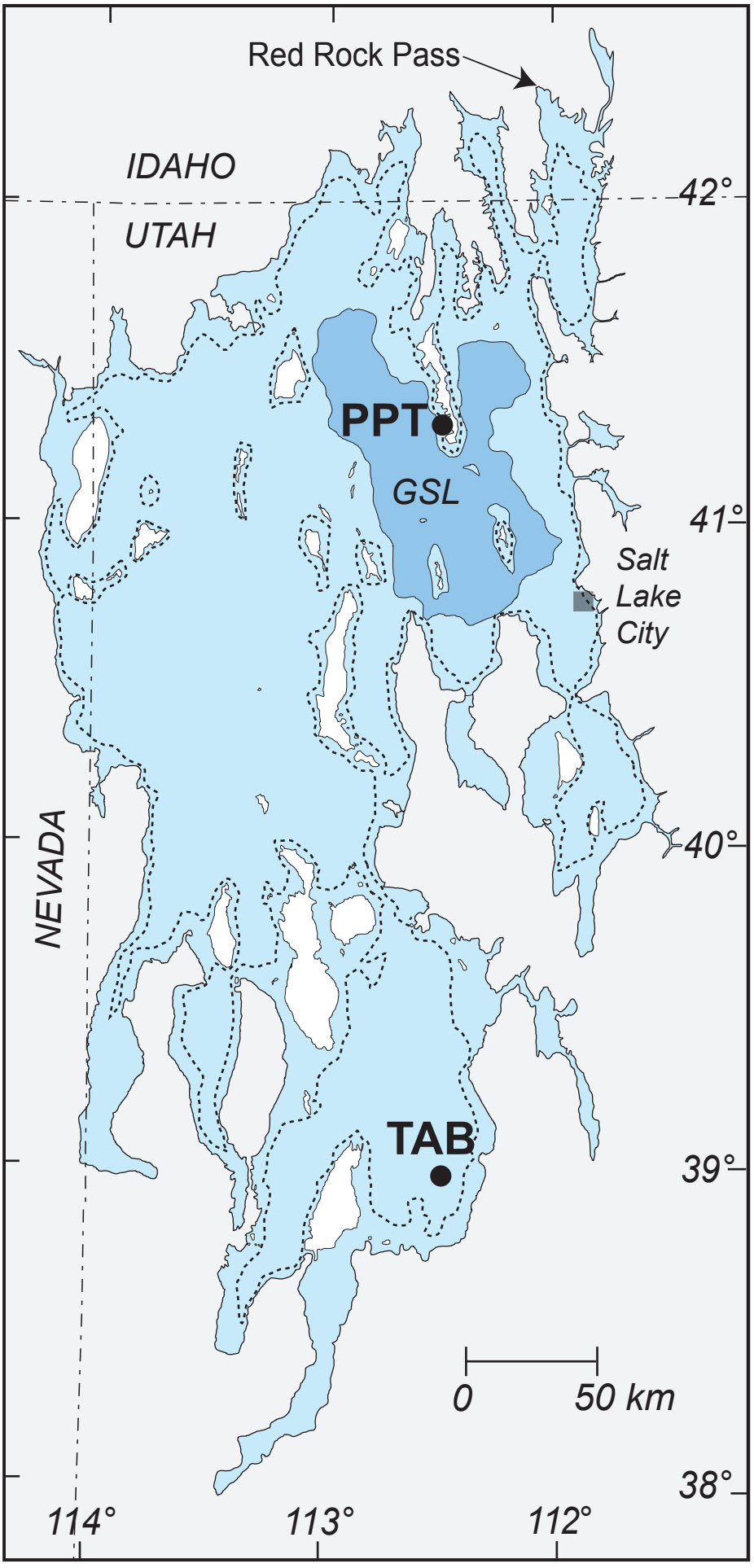

Maximum Extent of Lake Bonneville

Provo Shoreline Extent of Lake Bonneville

GSL Great Salt Lake

SAMPLING SITES

TAB Tabernacle Hill
PPT Promontory Point

Lifton et al.
CRONUS-Earth Lake Bonneville production rate calibration

Fig. 1

Figure 2

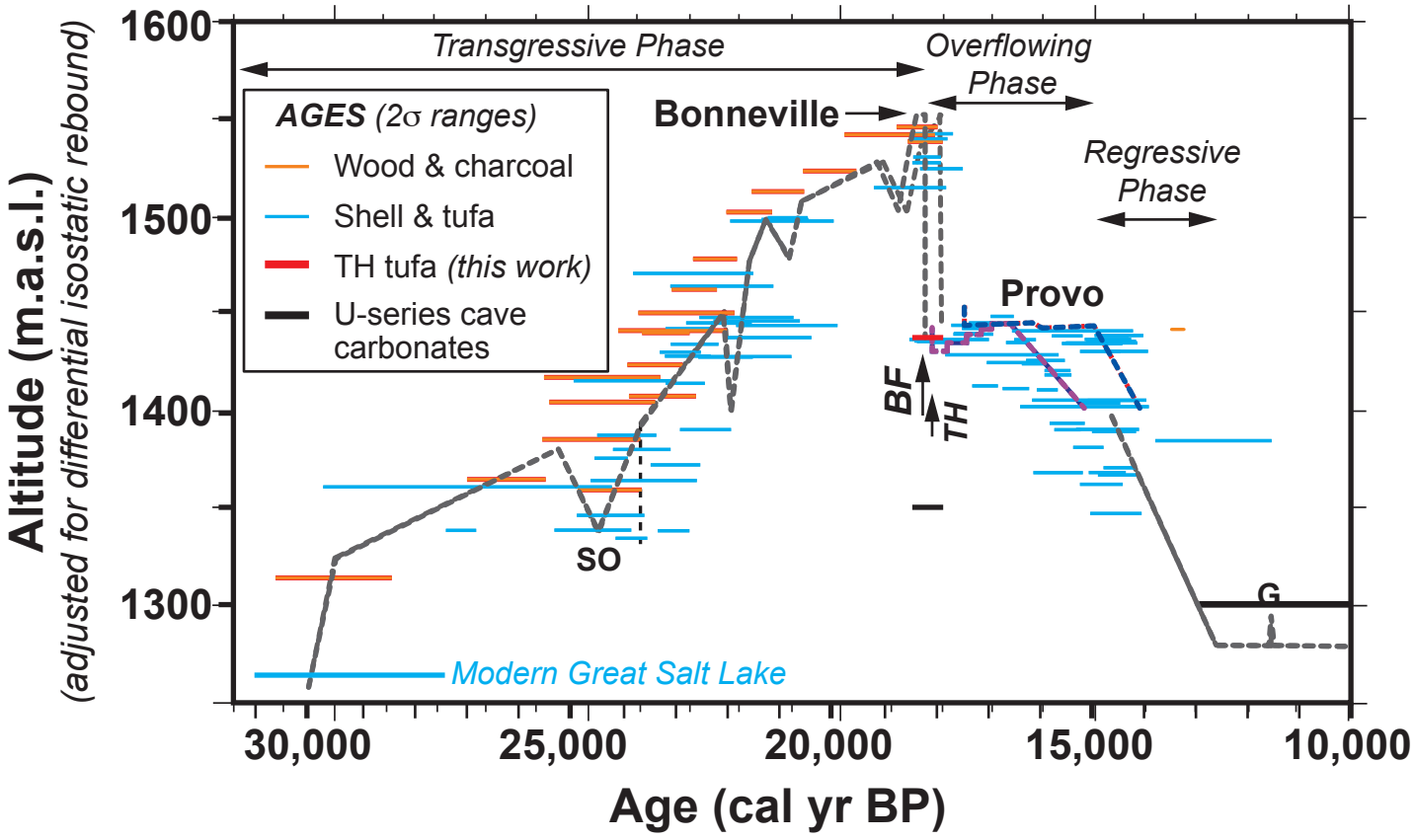

Lifton et al.
CRONUS-Earth Lake Bonneville production rate calibration

Fig. 2

Figure 3

Lifton et al.
CRONUS-Earth Lake Bonneville production rate calibration

Fig. 3

Figure 4

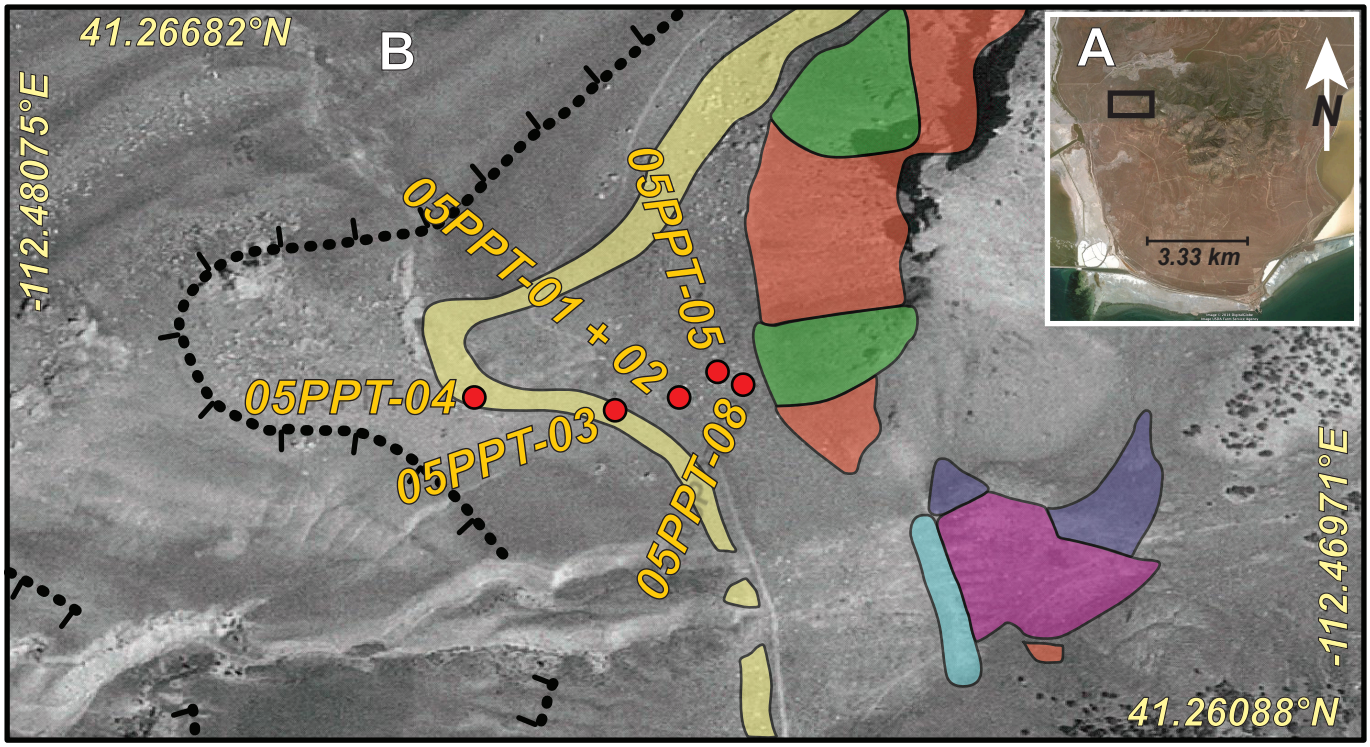

GEOMORPHIC UNITS

- Wave-Cut Bedrock
- Talus
- Boulder Berm
- Alluvial Fill
- Fan Delta
- Barrier Bar
- Major Slope Break

Lifton et al.
CRONUS-Earth Lake Bonneville production rate calibration

Fig. 4

Figure 5

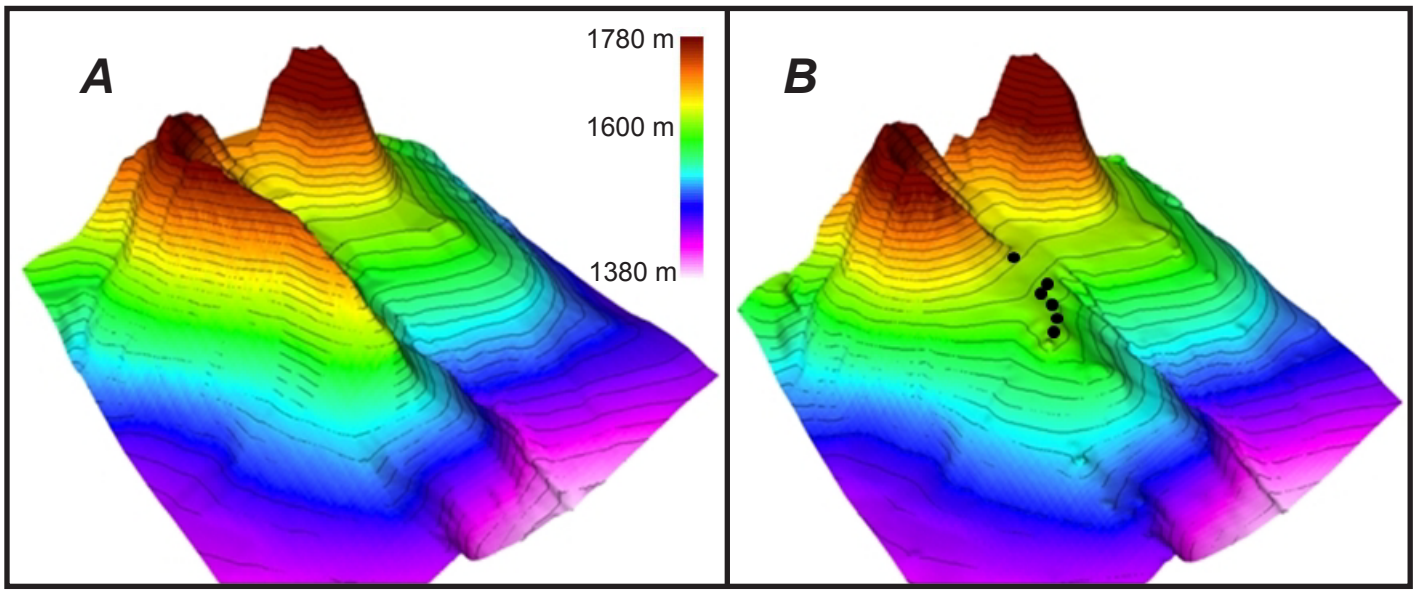

Lifton et al.
CRONUS-Earth Lake Bonneville production rate calibration

Fig. 5

Figure 6

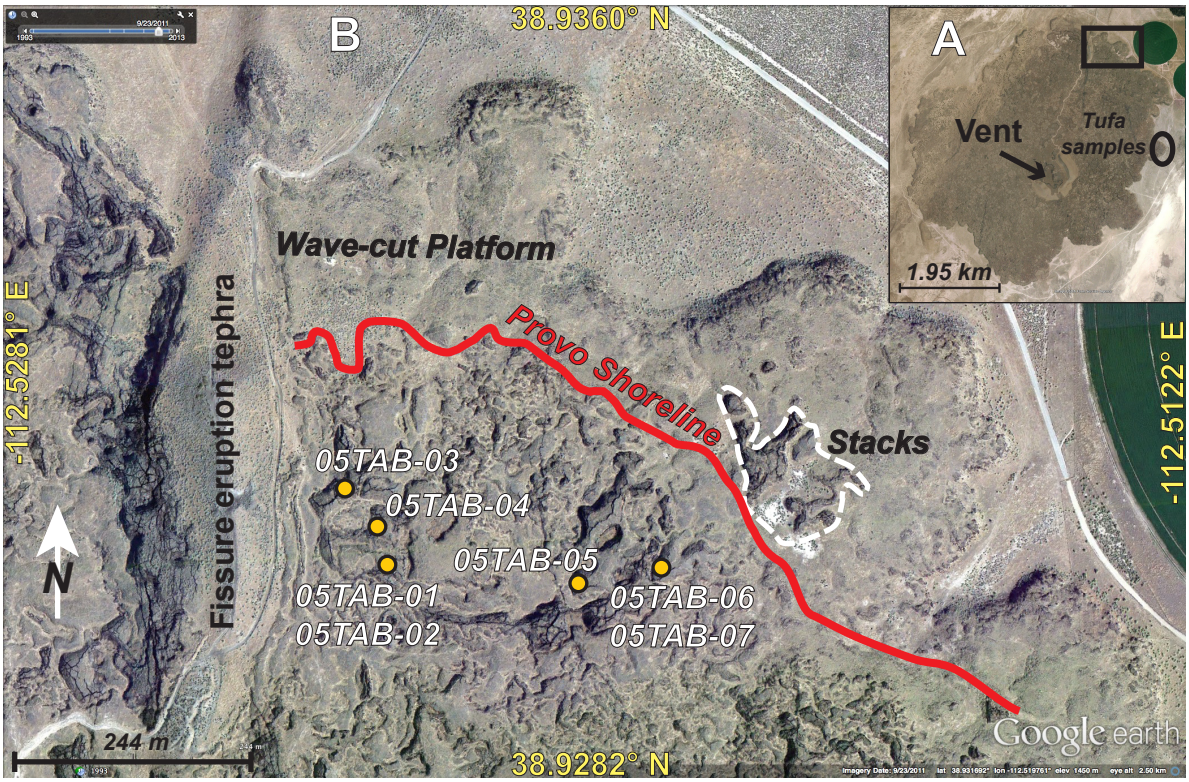

Lifton et al.
CRONUS-Earth Lake Bonneville production rate calibration

Fig. 6

Figure 7

Lifton et al.
CRONUS-Earth Lake Bonneville production rate calibration

Fig. 7

Figure 8

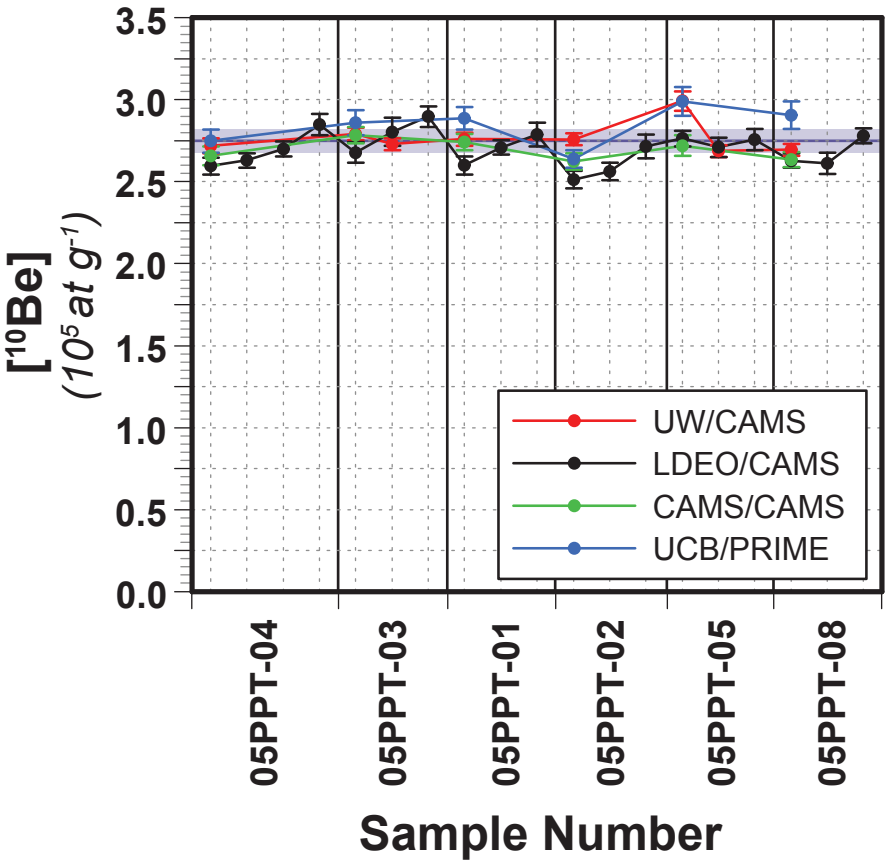

Lifton et al.
CRONUS-Earth Lake Bonneville production rate calibration

Fig. 8

Figure 9

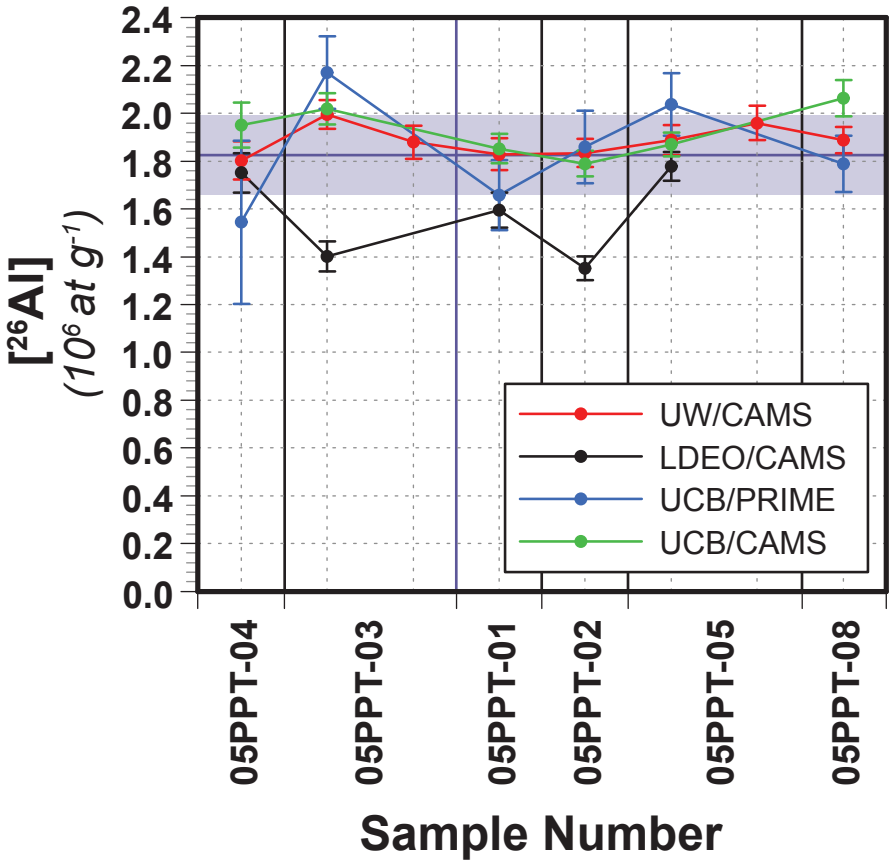

Lifton et al.
CRONUS-Earth Lake Bonneville production rate calibration

Fig. 9

Figure 10

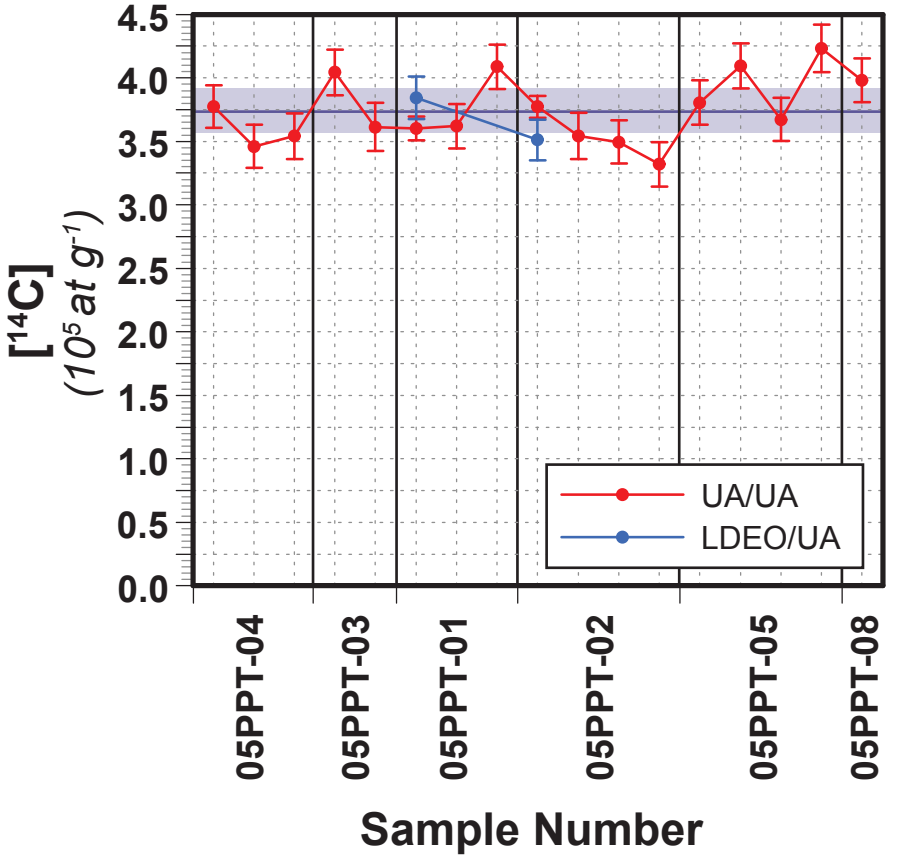

Lifton et al.
CRONUS-Earth Lake Bonneville production rate calibration

Fig. 10

Figure 11

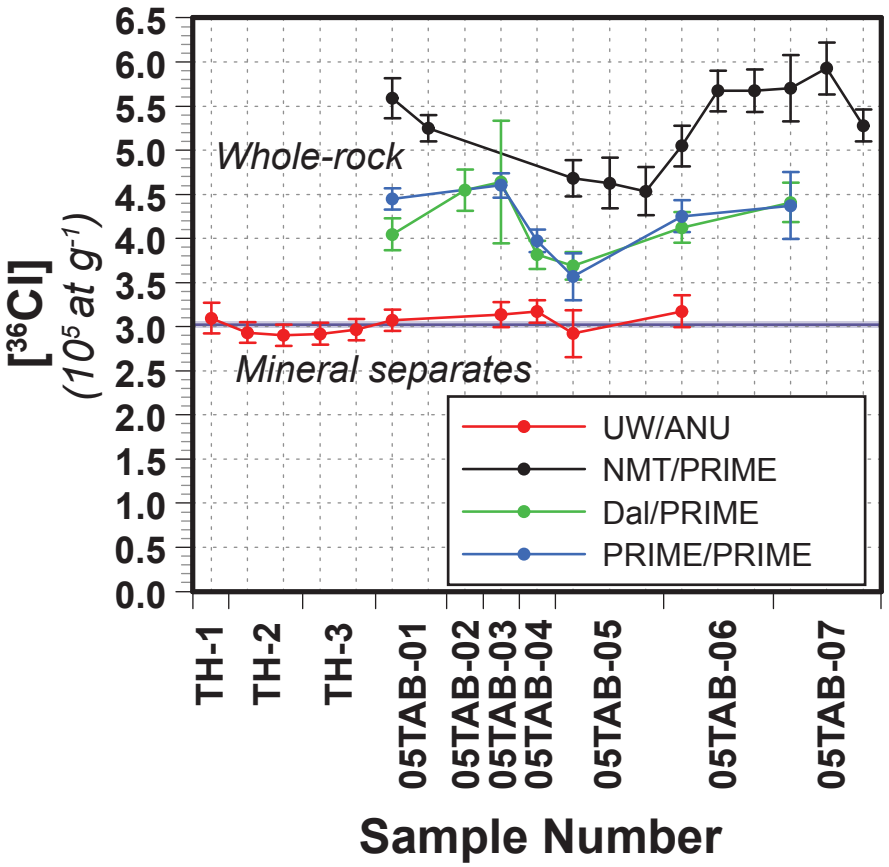

Lifton et al.
CRONUS-Earth Lake Bonneville production rate calibration

Fig. 11

Figure 12

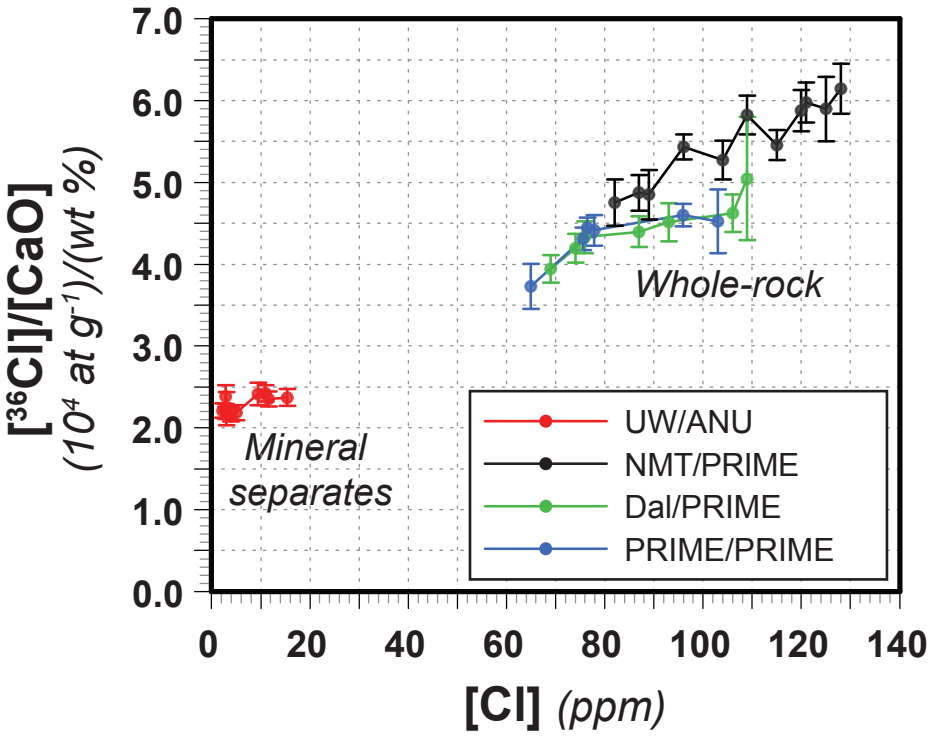

Lifton et al.
CRONUS-Earth Lake Bonneville production rate calibration

Fig. 12

Table 1 – New ^{14}C tufa measurements from Provo shore zone at Tabernacle Hill

Sample ID	Lab ID	^{14}C age *(yr BP)*	Cal ka Min	Cal ka Max
TAB 11/01 Top	AA-94394	14.57 ± 0.08	17.379	18.018
TAB 11/01 Bottom	AA-94395	14.76 ± 0.08	17.635	18.491
TAB 11/02 Top	AA-94396	14.95 ± 0.08	17.936	18.543
TAB 11/02 Bottom	AA-94397	14.97 ± 0.08	17.960	18.547
TAB 11/02 Top B	AA-94398	15.13 ± 0.08	18.027	18.613
TAB 11/03 Top	AA-94399	14.97 ± 0.08	17.960	18.547
TAB 11/03 Bottom	AA-94400	15.14 ± 0.08	18.026	18.622

Notes
Calibrated ages relative to present (1950)
Sample elevation = 1445 m

Table 2 – ^{10}Be, ^{26}Al, and ^{14}C sample measurements

Sample name	Latitude	Longitude	Elevation	Thickness	Density	Shielding correction	λ_{eff}	[^{10}Be]	[^{26}Al]	Lab/AMS	[^{14}C]	Lab/AMS
	(DD)	(DD)	(m)	(cm)	(g cm^{-3})		(g cm^{-2})	(10^5 at g^{-1})	(10^5 at g^{-1})		(10^5 at g^{-1})	
05PPT-01	41.2637	247.5247	1603	3	2.65	0.978	132	2.542±0.037	16.840±0.620	UW/CAMS	3.318±0.085	UA/UA
								2.394±0.052	14.690± 0.680	LDEO/CAMS	3.333±0.162	UA/UA
								2.495±0.040	--	LDEO/CAMS	3.764±0.161	UA/UA
								2.568±0.073	--	LDEO/CAMS	3.539±0.155	LDEO/UA
								2.526±0.045	--	CAMS/CAMS	--	--
								2.658±0.062	15.300±1.400	UCB/PRIME	--	--
								--	17.060±0.570	UCB/CAMS	--	--
05PPT-02	41.2637	247.5247	1603	3	2.65	0.994	142	2.594±0.034	17.250±0.560	UW/CAMS	3.547±0.083	UA/UA
								2.363±0.051	12.700±0.470	LDEO/CAMS	3.331±0.173	UA/UA
								2.408±0.051	--	LDEO/CAMS	3.286±0.159	UA/UA
								2.552±0.075	--	LDEO/CAMS	3.121±0.164	UA/UA
								2.467±0.046	--	CAMS/CAMS	3.303±0.151	LDEO/UA
								2.483±0.050	17.500±1.400	UCB/PRIME	--	--
								--	16.830±0.510	UCB/CAMS	--	--
05PPT-03	41.2636	247.5242	1600	3.5	2.65	0.962	123	2.490±0.035	17.800±0.540	UW/CAMS	3.607±0.160	UA/UA
								2.435±0.033	16.770±0.620	UW/CAMS	3.224±0.168	UA/UA
								2.390±0.057	12.500±0.560	LDEO/CAMS	--	--
								2.503±0.078	--	LDEO/CAMS	--	--
								2.585±0.062	--	LDEO/CAMS	--	--
								2.483±0.044	--	CAMS/CAMS	--	--
								2.552±0.067	19.400±1.400	UCB/PRIME	--	--
								--	18.000±0.580	UCB/CAMS	--	--
05PPT-04	41.2636	247.5231	1598	2.5	2.66	0.982	132	2.539±0.043	16.830±0.750	UW/CAMS	3.525±0.157	UA/UA
								2.424±0.047	16.350±0.760	LDEO/CAMS	3.231±0.159	UA/UA
								2.456±0.042	--	LDEO/CAMS	3.306±0.166	UA/UA
								2.521±0.043	--	LDEO/CAMS	--	--
								2.660±0.066	--	LDEO/CAMS	--	--
								2.481±0.054	--	CAMS/CAMS	--	--
								2.567±0.066	14.400±3.200	UCB/PRIME	--	--
								--	18.230±0.880	UCB/CAMS	--	--

Table 2 (cont'd) – ^{10}Be, ^{26}Al, and ^{14}C sample measurements

Sample name	Latitude	Longitude	Elevation	Thickness	Density	Shielding correction	λ_{eff}	[^{10}Be]	[^{26}Al]	Lab/AMS	[^{14}C]	Lab/AMS
	DD	*DD*	*m*	*cm*	*g cm^{-3}*		*g cm^{-2}*	*10^5 at g^{-1}*	*10^5 at g^{-1}*		*10^5 at g^{-1}*	
05PPT-05	41.2639	247.5250	1605	4	2.67	0.99	144	2.751±0.054	17.350±0.580	UW/CAMS	3.499±0.160	UA/UA
								2.470±0.033	18.010±0.660	UW/CAMS	3.764±0.161	UA/UA
								2.541±0.043	--	LDEO/CAMS	3.376±0.156	UA/UA
								2.492±0.054	16.340±0.550	LDEO/CAMS	3.892±0.173	UA/UA
								2.534±0.066	--	LDEO/CAMS	--	--
								2.501±0.057	--	CAMS/CAMS	--	--
								2.748±0.080	18.700±1.200	UCB/PRIME	--	--
								--	17.190±0.460	UCB/CAMS	--	--
05PPT-08	41.2638	247.5252	1606	2.5	2.68	0.986	143	2.536±0.035	17.770±0.530	UW/CAMS	3.745±0.161	UA/UA
								2.474±0.042	--	LDEO/CAMS	--	--
								2.459±0.061	--	LDEO/CAMS	--	--
								2.615±0.048	--	LDEO/CAMS	--	--
								2.480±0.044	--	CAMS/CAMS	--	--
								2.734±0.079	16.800±1.100	UCB/PRIME	--	--
								--	19.420±0.710	UCB/CAMS	--	--

Notes

Uncertainty in elevation assumed to be±10 m

Uncertainty on l_{eff} =±5 g cm^{-2}

Independent age of 18.36±0.3 ka before 2010

Uncertainty in thickness assumed to be±0.5 cm, assume no uncertainty in density

Uncertainty in shielding correction assumed to be ±0.005

Table 3 – ^{36}Cl sample measurements – Mineral Separates

Sample Name	Latitude *dd*	Longitude *dd*	Elevation *m*	Pore-water content *vol %*	Bulk density *g cm^{-3}*	Sample thickness *cm*	[^{36}Cl] *10^5 at g^{-1}*
TH-1f	–	–	–	0.01	2.12	5.5	2.86±0.16
TH-2f	–	–	–	0.01	2.12	5	2.73±0.11
TH-2c	–	–	–	0.01	2.12	5	2.70±0.11
TH-3f	–	–	–	0.01	2.12	7	2.64±0.11
TH-3c	–	–	–	0.01	2.12	7	2.68±0.11
05TAB-01	38.9301	247.4778	1463	0.01	2.80	4.5	2.82±0.11
05TAB-02	38.9301	247.4778	1455	0.01	2.80	4.5	–
05TAB-03	38.9308	247.4774	1461	0.01	2.11	4.5	2.94±0.13
05TAB-04	38.9305	247.4779	1457	0.01	1.92	4.5	2.99±0.12
05TAB-05	38.9299	247.4801	1455	0.01	2.00	4.5	2.75±0.25
05TAB-06	38.9301	247.4811	1457	0.01	2.18	4.5	2.97±0.17
05TAB-07	38.9301	247.4811	1457	0.01	2.50	4.5	–

Notes

TH samples collected in 1994 by John Stone – 38.93°N, 247.48°E, elevation 1455 m; 05TAB samples collected in 2005 by CRONUS investigators

TH samples prepared and analyzed at ANU; 05TAB samples prepared at University of Washington and analyzed at ANU

Uncertainty in elevation assumed to be±10 m

Assume l_{eff} = 147±5 g cm^{-2}

Independent age of 18.26±0.3 ka before 2010

Uncertainty in thickness assumed to be ±0.5 cm, bulk density uncertainty of 0.26 g cm^{-3}

Shielding correction assumed to be 1.000

Assume erosion rate of 1.0±1.0 mm/kyr

Assume pore water content (volume %) = 0.01±0.05%

Table 4 – ^{36}Cl sample elemental analyses – Mineral Separates

Sample Name	SiO_2	TiO_2	Al_2O_3	Fe_2O_3	MnO	MgO	CaO	Na_2O	K_2O	P_2O_5	H_2O-LOI	CO_2	Cl	B	Sm	Gd	U	Th	Cr	Li
	wt %	*wt %*	*wt %*	*wt %*	*wt %*	*wt %*	*wt %*	*wt %*	*wt %*	*wt %*	*wt %*	*wt %*	*ppm*	*ppm*	*ppm*	*ppm*	*ppm*	*ppm*	*ppm*	*ppm*
TH-1f	48.05±0.48	1.36±0.01 *0.08±0.0*	16.57±0.17	11.44±0.11 *0.60±0.01*	0.16±0.00	7.21±0.07	10.00±0.10 *12.98±0.13*	2.87±0.03	0.78±0.02 *0.24±0.0*	0.38±0.01	1.0±0.0	0.14±0.0	90±30 *2.9±0.9*	0.8±5	4.5±0.1	4.2±0.1	0.6±0.1	1.7±0.1	200±100	9.1±0.5
TH-2f	47.67±0.48	1.47±0.01 *0.08±0.0*	16.72±0.17	11.36±0.11 *0.60±0.01*	0.16±0.00	6.62±0.07	10.75±0.11 *13.28±0.13*	2.99±0.03	0.84±0.02 *0.23±0.0*	0.39±0.01	0.8±0.0	0.2±0.0	90±30 *2.2±0.8*	2.1±5	4.7±0.1	4.3±0.1	1.8±0.1	0.5±0.1	200±100	9.5±0.5
TH-2c	47.67±0.48	1.47±0.01 *0.08±0.0*	16.72±0.17	11.36±0.11 *0.60±0.01*	0.16±0.00	6.62±0.07	10.75±0.11 *13.28±0.13*	2.99±0.03	0.84±0.02 *0.23±0.0*	0.39±0.01	0.8±0.0	0.2±0.0	90±30 *5.0±1.0*	2.1±5	4.7±0.1	4.3±0.1	1.8±0.1	0.5±0.1	200±100	9.5±0.5
TH-3f	46.84±0.47	1.38±0.01 *0.06±0.0*	16.27±0.16	11.06±0.11 *0.60±0.01*	0.17±0.00	6.58±0.07	11.46±0.11 *13.48±0.13*	3.16±0.03	0.88±0.02 *0.23±0.0*	0.4±0.01	1.3±0.0	0.48±0.0	90±30 *3.9±1.1*	2.1±5	4.7±0.1	4.3±0.1	1.8±0.1	0.5±0.1	200±100	9.5±0.5
TH-3c	46.84±0.47	1.38±0.01 *0.06±0.0*	16.27±0.16	11.06±0.11 *0.60±0.01*	0.17±0.00	6.58±0.07	11.46±0.11 *13.48±0.13*	3.16±0.03	0.88±0.02 *0.23±0.0*	0.4±0.01	1.3±0.0	0.48±0.0	90±30 *2.8±0.9*	2.1±5	4.7±0.1	4.3±0.1	1.8±0.1	0.5±0.1	200±100	9.5±0.5
05TAB-01	50.30±0.50	1.30±0.01 *0.08±0.0*	18.50±0.19	8.15±0.08 *0.62±0.01*	0.11±0.00	5.37±0.05	10.00±0.10 *13.06±0.01*	3.23±0.03	0.8±0.02 *0.25±0.0*	0.18±0.00	1.6±0.0	0.35±0.0	90±10 *11.6±1.3*	10±5	3.2±0.1	3.7±0.1	0.5±0.0	1.5±0.2	170±50	5±5
05TAB-03	49.80±0.50	1.36±0.01 *0.08±0.0*	18.00±0.18	8.91±0.09 *0.63±0.01*	0.14±0.00	5.70±0.06	10.00±0.10 *13.23±0.13*	3.22±0.03	0.87±0.02 *0.23±0.0*	0.23±0.00	1.1±0.0	0.22±0.0	90±10 *15.4±2.4*	5±5	4.0±0.1	4.3±0.1	0.4±0.0	1.3±0.2	160±50	5±5
05TAB-04	49.11±0.49	1.57±0.02 *0.08±0.0*	16.47±0.16	12.00±0.12 *0.62±0.01*	0.18±0.00	7.90±0.08	9.22±0.09 *13.10±0.13*	3.15±0.03	0.69±0.01 *0.24±0.0*	0.24±0.00	0.0±0.0	0.0±0.0	90±30 *10.9±1.2*	5±5	3.0±0.5	3.0±0.5	0.5±0.2	1.5±1.0	200±100	5±5
05TAB-05	48.92±0.49	1.65±0.02 *0.07±0.0*	17.12±0.17	11.15±0.11 *0.61±0.01*	0.16±0.00	7.21±0.07	9.56±0.10 *13.07±0.13*	2.97±0.03	0.68±0.01 *0.23±0.0*	0.21±0.00	0.12±0.0	0.1±0.0	85±3 *3.0±1.2*	5±5	3.0±0.5	3.0±0.5	2.0±0.2	6.0±0.6	200±100	5±5
05TAB-06	49.14±0.49	1.67±0.02 *0.08±0.0*	16.93±0.17	11.17±0.11 *0.61±0.01*	0.16±0.00	6.97±0.07	9.63±0.10 *13.15±0.13*	3.03±0.03	0.75±0.02 *0.24±0.0*	0.27±0.01	0.13±0.0	0.12±0.0	110±10 *9.4±5.1*	5±5	3.0±0.5	3.0±0.5	4.0±0.4	1.0±1.0	200±100	5±5

Notes

All analyses are bulk rock except for those in italics, which indicate target compositions

Table 5 – ^{36}Cl sample measurements – Whole-rock

Lab	Sample Name	[^{36}Cl] 10^5 at g^{-1}
NMT	05TAB-01	5.13±0.21
	05TAB-01	4.82±0.14
	05TAB-05	4.40±0.20
	05TAB-05	4.35±0.27
	05TAB-05	4.27±0.26
	05TAB-06	4.72±0.21
	05TAB-06	5.31±0.22
	05TAB-06	5.31±0.23
	05TAB-07	5.28±0.35
	05TAB-07	5.49±0.27
	05TAB-07	4.89±0.17
Dalhousie (Dal)	05TAB-01	3.71±0.17
	05TAB-02	4.17±0.22
	05TAB-03	4.35±0.65
	05TAB-04	3.60±0.15
	05TAB-05	3.47±0.15
	05TAB-06	3.86±0.16
	05TAB-07	4.08±0.20
PRIME	05TAB-01	4.08±0.11
	05TAB-03	4.32±0.13
	05TAB-04	3.74±0.12
	05TAB-05	3.35±0.25
	05TAB-06	3.98±0.17
	05TAB-07	4.05±0.35

Notes

Uncertainty in elevation assumed to be±10 m

Assume l_{eff} = 147±5 g cm^{-2}

Independent age of 18.26±0.3 ka before 2010

Uncertainty in thickness assumed to be±0.5 cm, bulk density uncertainty of 0.26 g cm^{-3}

Shielding correction assumed to be 1.000±0.005

Assume erosion rate of 1.0±0.5 mm/kyr

Assume pore water content (volume %) = 0.01±0.05% (Dalhousie assumed 0.05±0.05%)

Table 6 – ^{36}Cl sample elemental analyses – Whole-rock

Lab	Sample Name	SiO_2	TiO_2	Al_2O_3	Fe_2O_3	MnO	MgO	CaO	Na_2O	K_2O	P_2O_5	H_2O- LOI	CO_2	Cl	B	Sm	Gd	U	Th	Cr	Li
		wt %	*wt %*	*wt %*	*wt %*	*wt %*	*wt %*	*wt %*	*wt %*	*wt %*	*wt %*	*wt %*	*wt %*	*ppm*	*ppm*	*ppm*	*ppm*	*ppm*	*ppm*	*ppm*	*ppm*
NMT	05TAB-01	49.27±0.10	1.63±0.10	17.24±0.10	11.02±0.10	0.16±0.10	6.94±0.10	9.60±0.10	3.07±0.10	0.75±0.10	0.21±0.10	0.00±0.30	0.00±0.20	108.57±1.80	0.0±5.0	3.0±0.1	3.00±0.10	0.00±0.20	3.00±0.20	0.00±50	0.0±5.0
	05TAB-01	49.16±0.10	1.64±0.10	17.32±0.10	10.94±0.10	0.16±0.10	6.72±0.10	9.66±0.10	3.07±0.10	0.76±0.10	0.21±0.10	0.22±0.30	0.00±0.20	96.23±1.55	0.0±5.0	3.0±0.1	3.00±0.10	0.00±0.20	3.00±0.20	0.00±50	0.0±5.0
	05TAB-05	48.99±0.10	1.66±0.10	17.19±0.10	11.11±0.10	0.16±0.10	7.10±0.10	9.61±0.10	3.00±0.10	0.68±0.10	0.22±0.10	0.14±0.30	0.00±0.20	86.61±1.22	0.0±5.0	3.0±0.1	3.00±0.10	2.00±0.20	6.00±0.20	0.00±50	0.0±5.0
	05TAB-05	48.89±0.10	1.63±0.10	17.05±0.10	11.14±0.10	0.16±0.10	7.32±0.10	9.54±0.10	2.98±0.10	0.68±0.10	0.21±0.10	0.26±0.30	0.00±0.20	88.64±1.39	0.0±5.0	3.0±0.1	3.00±0.10	2.00±0.20	6.00±0.20	0.00±50	0.0±5.0
	05TAB-05	48.88±0.10	1.65±0.10	17.11±0.10	11.21±0.10	0.16±0.10	7.22±0.10	9.54±0.10	2.93±0.10	0.67±0.10	0.21±0.10	0.27±0.30	0.00±0.20	82.38±4.63	0.0±5.0	3.0±0.1	3.00±0.10	2.00±0.20	6.00±0.20	0.00±50	0.0±5.0
	05TAB-06	48.99±0.10	1.67±0.10	16.79±0.10	11.28±0.10	0.16±0.10	7.04±0.10	9.57±0.10	2.99±0.10	0.75±0.10	0.27±0.10	0.34±0.30	0.00±0.20	103.53±1.52	0.0±5.0	3.0±0.1	3.00±0.10	4.00±0.20	0.00±0.20	0.00±50	0.0±5.0
	05TAB-06	48.80±0.10	1.65±0.10	16.74±0.10	11.30±0.10	0.16±0.10	7.09±0.10	9.49±0.10	3.00±0.10	0.74±0.10	0.27±0.10	0.62±0.30	0.00±0.20	120.76±1.69	0.0±5.0	3.0±0.1	3.00±0.10	4.00±0.20	0.00±0.20	0.00±50	0.0±5.0
	05TAB-06	49.18±0.10	1.65±0.10	16.93±0.10	11.14±0.10	0.16±0.10	7.07±0.10	9.65±0.10	3.02±0.10	0.74±0.10	0.27±0.10	0.04±0.30	0.00±0.20	120.44±1.90	0.0±5.0	3.0±0.1	3.00±0.10	4.00±0.20	0.00±0.20	0.00±50	0.0±5.0
	05TAB-07	49.24±0.10	1.68±0.10	17.12±0.10	10.91±0.10	0.16±0.10	6.50±0.10	9.67±0.10	3.09±0.10	0.87±0.10	0.27±0.10	0.33±0.30	0.00±0.20	125.05±2.17	10.0±5.0	5.7±0.1	5.70±0.10	2.00±0.20	6.00±0.20	0.00±50	0.0±5.0
	05TAB-07	49.40±0.10	1.67±0.10	17.02±0.10	11.03±0.10	0.16±0.10	6.69±0.10	9.65±0.10	3.10±0.10	0.87±0.10	0.27±0.10	0.00±0.30	0.00±0.20	128.20±2.24	10.0±5.0	5.7±0.1	5.70±0.10	2.00±0.20	6.00±0.20	0.00±50	0.0±5.0
	05TAB-07	49.41±0.10	1.69±0.10	17.11±0.10	10.97±0.10	0.16±0.10	6.58±0.10	9.68±0.10	3.13±0.10	0.87±0.10	0.27±0.10	0.00±0.30	0.00±0.20	115.48±1.94	10.0±5.0	5.7±0.1	5.70±0.10	2.00±0.20	6.00±0.20	0.00±50	0.0±5.0
Dal	05TAB-01	48.96±0.10	1.60±0.10	17.01±0.10	11.74±0.10	0.18±0.10	6.75±0.10	9.34±0.10	3.04±0.10	0.78±0.10	0.23±0.10	0.27±0.30	0.00±0.20	76.37±1.47	1.0±5.0	3.3±0.1	3.82±0.10	0.38±0.20	1.30±0.20	340.40±50	1.0±5.0
	05TAB-02	49.95±0.10	1.71±0.10	18.15±0.10	9.89±0.10	0.15±0.10	5.37±0.10	10.07±0.10	3.25±0.10	0.85±0.10	0.19±0.10	0.23±0.30	0.00±0.20	93.43±2.88	1.0±5.0	3.8±0.1	3.99±0.10	0.34±0.20	1.40±0.20	409.29±50	1.0±5.0
	05TAB-03	48.61±0.10	1.53±0.10	16.70±0.10	11.63±0.10	0.17±0.10	7.26±0.10	9.19±0.10	3.03±0.10	0.86±0.10	0.35±0.10	0.56±0.30	0.00±0.20	108.61±1.84	20.0±5.0	4.2±0.1	4.13±0.10	0.53±0.20	1.90±0.20	408.07±50	1.0±5.0
	05TAB-04	48.67±0.10	1.51±0.10	16.98±0.10	11.45±0.10	0.17±0.10	7.21±0.10	9.10±0.10	2.88±0.10	0.69±0.10	0.23±0.10	1.02±0.30	0.00±0.20	74.50±1.35	10.0±5.0	3.6±0.1	3.60±0.10	0.35±0.20	1.50±0.20	405.25±50	1.0±5.0
	05TAB-05	49.20±0.10	1.59±0.10	17.20±0.10	11.13±0.10	0.16±0.10	7.01±0.10	9.35±0.10	2.95±0.10	0.70±0.10	0.22±0.10	0.34±0.30	0.00±0.20	68.81±1.36	10.0±5.0	3.1±0.1	3.57±0.10	0.36±0.20	1.20±0.20	408.07±50	1.0±5.0
	05TAB-06	49.05±0.10	1.61±0.10	16.78±0.10	11.69±0.10	0.17±0.10	6.96±0.10	9.38±0.10	2.98±0.10	0.80±0.10	0.32±0.10	0.12±0.30	0.00±0.20	87.44±1.45	10.0±5.0	4.3±0.1	4.37±0.10	0.53±0.20	1.90±0.20	341.76±50	1.0±5.0
	05TAB-07	49.21±0.10	1.63±0.10	16.96±0.10	11.41±0.10	0.17±0.10	6.68±0.10	9.53±0.10	3.11±0.10	0.89±0.10	0.33±0.10	0.09±0.30	0.00±0.20	106.32±1.81	10.0±5.0	4.6±0.1	4.54±0.10	0.54±0.20	1.80±0.20	407.26±50	1.0±5.0
PRIME	05TAB-01	50.30±0.10	1.30±0.10	18.50±0.10	8.15±0.10	0.11±0.10	5.37±0.10	10.00±0.10	3.23±0.10	0.83±0.10	0.18±0.10	1.60±0.30	0.35±0.20	76.51±10.00	10.0±5.0	3.2±0.1	3.70±0.10	0.50±0.20	1.50±0.20	170.00±50	5.0±5.0
	05TAB-03	49.80±0.10	1.36±0.10	18.00±0.10	8.91±0.10	0.14±0.10	5.70±0.10	10.00±0.10	3.22±0.10	0.87±0.10	0.23±0.10	1.10±0.30	0.22±0.20	95.88±10.00	5.0±5.0	4.0±0.1	4.30±0.10	0.40±0.20	1.30±0.20	160.00±50	5.0±5.0
	05TAB-04	49.11±0.10	1.57±0.10	16.47±0.10	12.00±0.10	0.18±0.10	7.90±0.10	9.22±0.10	3.15±0.10	0.69±0.10	0.24±0.10	0.00±0.30	0.00±0.20	75.61±30.00	5.0±5.0	3.0±0.1	3.00±0.10	0.50±0.20	1.50±0.20	200.00±50	5.0±5.0
	05TAB-05	48.92±0.10	1.65±0.10	17.12±0.10	11.15±0.10	0.16±0.10	7.21±0.10	9.56±0.10	2.97±0.10	0.68±0.10	0.21±0.10	0.12±0.30	0.10±0.20	65.00±3.00	5.0±5.0	3.0±0.1	3.00±0.10	2.00±0.20	6.00±0.20	200.00±50	5.0±5.0
	05TAB-06	49.14±0.10	1.67±0.10	16.93±0.10	11.17±0.10	0.16±0.10	6.97±0.10	9.63±0.10	3.03±0.10	0.75±0.10	0.27±0.10	0.13±0.30	0.12±0.20	77.83±10.00	5.0±5.0	3.0±0.1	3.00±0.10	4.00±0.20	1.00±0.20	200.00±50	5.0±5.0
	05TAB-07	49.24±0.10	1.68±0.10	17.12±0.10	10.91±0.10	0.16±0.10	6.50±0.10	9.67±0.10	3.09±0.10	0.87±0.10	0.27±0.10	0.33±0.30	0.00±0.20	103±2.17	10.0±5.0	5.7±0.1	5.70±0.10	2.00±0.20	6.00±0.20	0.00±50	0.0±5.0

Notes

All analyses are bulk rock

Appendices

Click here to download Supplementary Data: BonnevilleCalibrationAppendixRev.pdf